2002-06

A Neural Model of How the Cortical Subplate Coordinates the Laminar Development of Orientation and Ocular Dominance Maps

A neural model of how the cortical subplate coordinates the laminar development of orientation and ocular dominance maps

Stephen Grossberg and Aaron Seitz

June, 2002

Technical Report CAS/CNS-02-006

Boston University Center for Adaptive Systems and

Department of Cognitive and Neural Systems

677 Beacon Street

Boston, MA 02215

A Neural Model of How the Cortical Subplate Coordinates the Laminar Development of Orientation and Ocular Dominance Maps

Stephen Grossberg[1] and Aaron Seitz[1*]

Department of Cognitive and Neural Systems
and
Center for Adaptive Systems
Boston University
677 Beacon Street, Boston, MA 02215, USA
June, 2002
Email: steve@cns.bu.edu, aseitz@bu.edu

Abbreviated title: Cortical subplate coordinates V1 maps and columns

June 2002

Technical Report CAS/CNS-02-006

*Authorship in alphabetical order

Supported in part by: Air Force Office of Scientific Research (AFOSR F49620-98-1-0108 and F49620-01-1-0397), the Defense Advanced Research Projects Agency and the Office of Naval Research (ONR N00014-95-1-0409), the National Science Foundation (NSF IIS-97-20333), and the Office of Naval Research (ONR N00014-01-1-0624).

Abstract

How is development of cortical maps in V1 coordinated across cortical layers? Previous neural models propose how maps of orientation (OR), ocular dominance (OD), and related properties develop in V1. These models show how spontaneous activity, before eye opening, combined with correlation learning and competition, can generate map structures similar to those found *in vivo*. These models have not discussed laminar architecture or how cells develop their connections across cortical layers. This is an important problem since anatomical evidence shows that clusters of horizontal connections form, between iso-oriented regions, in layer 2/3 before being innervated by layer 4 afferents. How are orientations in different layers aligned before these connections form? Anatomical evidence demonstrates that thalamic afferents wait in the subplate for weeks before innervating layer 4. Other evidence shows that ablation of the cortical subplate interferes with the development of OR and OD columns. The model proposes how the subplate develops OR and OD maps, which then entrain the development of maps in other lamina. Mechanisms which have been proposed to develop OR and OD maps in earlier models of the cortical plate can drive their development in the model subplate. The model demonstrates how these maps may then be transferred to layer 4 by a known transient subplate-to-layer 4 circuit. The model subplate also guides the early clustering of horizontal connections in layer 2/3, and the formation of interlaminar circuitry. It is shown how layer 6 develops and helps to stabilize the network when the subplate atrophies. Finally the model clarifies how BDNF manipulations may influence cortical development.

KEYWORDS: cortical development, cortical subplate, V1, orientation map, ocular dominance map, cortical layers, BDNF

Topographic maps have been found in visual (Duffy et al., 1998; Tootell et al., 1982, 1998), auditory (Komiya and Eggermont, 2000; Stanton and Harrison, 2000), somatosensory (Dykes et al., 1980; Grinvald et al.,1986; Wallace and Stein, 1996) and motor (Chakrabarty and Martin, 2000; Munoz et al., 1991; Nieoullon and Rispal-Padel, 1976) thalamic and cortical areas. In V1, cells tuned to orientation and ocular dominance are found within its map (Blasdel, 1992a, 1992b; Crair et al., 1997a, 1997b; Hubener et al., 1997). Cortical columns show consistent tuning for orientation and ocular dominance along vertical penetrations of this map (Hubel and Wiesel, 1974). An important step toward understanding the brain, and in building computational models thereof, is how these columnar maps emerge.

A rich modeling literature addresses the development of orientation and ocular dominance columns in V1 (Grossberg, 1976; Kohonen, 1982; Linsker 1986a, 1986b, 1986c; Miller et al., 1989; Olson and Grossberg, 1998; Rojer and Schwartz, 1990; Swindale, 1980, 1992; von der Malsburg, 1973; Willshaw and von der Malsburg, 1976). Most models do not, however, address how maps are distributed or coordinated across the layered circuits of striate cortex. Furthermore, these models typically do not address the development of key properties, such as the clusters of horizontal connections found in layers 2/3 and 5 (Gilbert and Wiesel, 1983, 1985, 1989, Katz et al., 1989, 1989; McGuire et al., 1991; Ts'o et al., 1986; Sincich and Blasdel, 2001; Schmidt et al., 1997a, 1997b, 1999). These connections have been shown to preferentially target other cells of similar ocularity and orientation tuning (Bosking et al., 1997; Yoshioka et al., 1996).

A challenge to modeling is that the orientation maps in layers 4 and 6, and the crude clustering in layers 2/3 and 5, begin to develop before there are interlaminar connections to coordinate the formation of such maps across layers (Callaway and Katz, 1992). These initial preferences are maintained as patterned vision refines them (Callaway and Katz, 1990, 1991). How are these initial preferences coordinated in the absence of interlaminar connections? This article proposes that this problem is solved by the cortical subplate (Allendoerfer, 1994; Ghosh et al., 1994, 1995; Luskin and Shatz, 1985; McAllister, 1999). The subplate serves as an early target of thalamocortical connections and in turn makes connections throughout the developing cortical plate (Ghosh and Shatz, 1993; McConnell et al., 1994). Furthermore, ablation of the subplate eliminates the formation of cells tuned to orientation (Kanold et al., 2001) and ocular dominance maps (Ghosh and Shatz, 1992).

A new neural model describes development of orientation tuning and ocular dominance columns, clustered horizontal connections, and interlaminar connections. Some of these results were briefly reported in Seitz and Grossberg (2001, 2002). Modeling simulations emulate the order of biological development. Inputs from the Lateral Geniculate Nucleus (LGN) to the cortical subplate induce a map, which is taught to the other cortical layers. Interlaminar connections next develop and the model is shown to be stable after subplate atrophy. Finally, patterned vision segregates ON and OFF receptive fields. The model also clarifies how BDNF manipulations may influence map development (Cabelli et al., 1995, 1997).

Materials and Methods

This section summarizes relevant properties of the laminar organization of cortex, the cortical subplate, orientation tuning, ocular dominance columns, and clustered horizontal connections before introducing the model and describing the mathematical equations used in the

simulations. The Results section compares simulations of the various modeling stages with physiological and anatomical data.

Laminar Organization of Cortex

Neocortex has an intricate design that exhibits a characteristic organization consisting of six layers (Brodmann 1909). Each of these layers differs in their configuration of cell types, and the makeup of the layers differs across brain areas. In V1, layers 4 and 6 receive inputs from the LGN. Layers 2/3 and 5 exhibit long-range horizontal connections between cells in their respective layers.

A fundamental question in cortical development is how do the receptive field properties of the cortical layers develop? Key to this debate is that the very young cortex looks similar across different brain regions, yet the adult cortex shows remarkable differences. For example, V1 has a prominent layer 4, consisting of multiple sublaminae, whereas motor cortex has almost no layer 4. Competing "Protomap" and "Protocortex" theories have emerged with different explanations of how cortex differentiates (Donoghue and Rakic, 1999). The "Protocortex" theory suggests that different cortical areas have different innate make-ups of patterning molecules, which cause differentiation after cell migration. The "Protomap" theory suggests that the cortex differentiates due to differences found in their thalamic inputs.

A different question is how the layers are differentiated from each other. Cortical cells migrate from the ventricular zone into the cortical plate in an inward out manner: layer 6, then 5, then onwards until layer 2 forms. Cells in different layers come from different generations of cell divisions in the ventricular zone, and have different molecular make-ups (McAllister et al., 1997). Studies in culture demonstrate that cells of each generation innately "know" to what layer to send their axons and dendrites (McConnell and Kaznowski, 1991), although the specification of connections to sublaminae and within layers requires activity-dependent refinement (Callaway, 1998b).

Subplate

The cortical subplate is traditionally thought of as a transient cortical area underlying the cortical plate that is responsible for proper target recognition of the thalamocortical connections. If the V1 subplate is ablated before the LGN growth cones contact cortex, the LGN efferents will grow past V1 and instead innervate other cortical areas (Ghosh and Shatz, 1993). Afferents from the LGN "wait" in the cortical subplate for a period of weeks before growing into the cortical plate (Ghosh and Shatz, 1992, 1994). If the subplate is ablated shortly after the LGN grows into layer 4, ocular dominance columns (Ghosh and Shatz, 1992) and orientation tuning (Kanold et al., 2001) fail to develop. There exist reciprocal connections between the subplate and layer 4 (Ghosh, 1995). There also exist connections from the subplate to layer 1 (Allendoerfer and Shatz, 1994). Cells in layers 2/3 and 5 have apical dendrites in layer 1 (Callaway, 1998b). Connections also exist from most cortical layers to the subplate (Callaway, 1998b). Thus, circuits exist by which early activity in each of the layers of the cortical plate may be driven and coordinated by the subplate.

[Insert Figure 1, about here]

The present model proposes that the subplate contains sufficient circuitry to develop its own ocular dominance and orientation maps; namely, lateral excitation and inhibition (see Figure 1), spontaneous inputs from the thalamus, and correlation learning (Grossberg and Olson, 1994). When the LGN efferents grow into layer 4, the subplate also makes connections in layer 4 and correlations

from the subplate guide the growth of the LGN-to-layer 4 connections and result in layer 4 learning the map induced by the subplate inputs. Likewise, the subplate is the main source of drive for layer 2/3, via the apical dendrites of the cells in layer 1, and the correlations from the subplate guide the clustering of horizontal connections in this layer. The correlations provided by the subplate across layers guides the development of vertical interlaminar connections.

Orientation Tuning

Hubel and Wiesel discovered cells in area 17 (V1) of the cat that fire in preference to bars of a particular orientation (Hubel and Wiesel, 1959). The preferred orientation of V1 cells varies smoothly in tangential penetrations and remains mostly constant in vertical penetrations (Hubel and Wiesel 1962). Hubel and Wiesel (1962) proposed that orientation tuning originates from an oriented pattern of input from the LGN. Multiple LGN cells, with spatially offset receptive fields, terminate onto a single V1 simple cell. Other researchers have verified that the input from the LGN to an individual cortical simple cell are oriented along the same axis as the preferred orientation of that cell (Chapman et al., 1991; Reid and Alonso, 1995). The sufficiency of this oriented input to explain data of orientation selectivity is still controversial (Anderson et al., 2000; Carandini and Ringach, 1997; Ferster and Miller, 2000).

The clearest data concerning the development of orientation selectivity comes from two sources: optical imaging and electrophysiology. The data from optical imaging indicates global properties of orientation maps, but since this method necessarily averages the response of many cells within and across layers, it does not give much insight into the tuning curves or receptive fields of individual cells, or of differences across cortical layers. The data from electrophysiology provides tuning curves of single cells, can be used to derive receptive fields, and can look at laminar differences, but does not give clear data on the global organization of the properties of these cells.

Crair et al. (1998) examined the time course of the development of orientation selectivity in the cat. They found that regular orientation maps were in place by the end of the second postnatal week (W2). At this point, the response from visual input to the contralateral eye was much stronger than that to the ipsilateral eye, but the orientation maps were similar between the two eyes. The orientation map continued to be refined until W4, but the overall pattern of the map remained largely constant.

Albus and Wolf (1984) conducted a laminar analysis of the development of orientation tuning in the cat. They discovered a number of orientationally tuned cells at the time of eye opening and that, within a few days of patterned vision, both the responsiveness and proportion of orientationally tuned cells increased. They also found that layers 4 and 6 developed light responsiveness and tuning a week or two before the cells in layers 2/3 and 5 become responsive and tuned. During the next few weeks, the proportion of orientationally tuned cells increased dramatically, reaching adult levels by week 6.

Ocular Dominance

Hubel and Wiesel also found that a given cell in V1 typically prefers input from one or the other eye (ocular dominance) (Hubel and Wiesel, 1962). They found that ocular dominance also varies smoothly in tangential penetrations and remains constant in vertical penetrations. In the input layers of V1, cells are predominantly monocular, and in the output layers, cells are often binocular with a preference for a given eye. Injecting [^{3}H]-Proline into a single eye revealed alternating stripes

of cortex connected to one or the other eye (Shatz et al., 1977). Such ocular dominance columns have been identified in cats, ferrets, new world monkeys, and humans.

Older studies using [^{3}H]-Proline typically first identified ocular dominance columns (ODCs) in the third or fourth weeks of life. Since cats open their eyes early in the second week, researchers concluded that the patterned activity was necessary for the formation of ODCs. More recently, optical imaging has been used to identify ODCs that form by the second postnatal week (Crair et al., 2001). It is possible that ODCs exist even earlier than this, as the signal in optical imaging is less reliable in the deeper layers. The data from Albus and Wolf (1984) indicate that the first visibly responsive cells are monocular and respond to either eye. However, their data do not show the organization of these cells in each layer.

ON and OFF Receptive Fields

Ganglion cells in the retina, the primary retinal output cells, include ON cells that respond to increments of light in the center of their receptive fields, and OFF cells that respond to decrements of light their receptive fields centers. These cell types terminate in different sublamina of the LGN (Weliky and Katz, 1999) and in different subregions of the receptive fields of cortical simple cells (Alonso et al., 2001; Reid and Alonso, 1995). The organization of ON and OFF subregions are an important property of cells in V1 and play a role in the degree of orientation tuning, direction tuning, and construction of complex cells, among other properties.

The receptive field structure of V1 cells changes dramatically over the course of the first few weeks. Young cells have receptive fields that are largely monocular and dominated by contralateral eye inputs (Crair et al., 1998). These cells typically have a single excitatory region dominated by OFF-cell input (Albus and Wolf, 1984). By the fourth week, the typical cell has both ON and OFF regions and is responsive to inputs from each eye. It is likely that the increase of orientation selectivity occurring through the fourth week (Albus and Wolf, 1984; Crair et al., 1998) is due to coordination of OFF and ON regions of the receptive field.

Horizontal Connections in Layer 2/3

Layer 2/3 of V1 contains cells that have long-range lateral connections. These intralaminar connections are clustered and primarily connect cells of similar ocular dominance (Löwel and Singer, 1992) and orientation preference (Ts'o et al., 1986). There is also some evidence that the long axis of these interlaminar connections is in the same direction of the preferred orientation of the cells (Grossberg and Mingolla, 1985; Sincich and Blasdel, 2001; Schmidt et al., 1997a, 1997b, 1999). These clusters are identified by applying Rhodamine (an anterograde/retrograde tracer) in layers 2/3 or 5 (Gilbert and Wiesel, 1983). This tracer stains the cell bodies of cells with synaptic connections to the stained area. These horizontal connections are used to explain perceptual grouping and attentional effects in models of visual processing (Grossberg and Raizada, 2000; Grossberg and Williamson, 2001).

Clustered horizontal connections in layer 2/3 provide important clues about how the early stages of the orientation map develop. Such connections are found in the second week (P8), before the age of visual responsiveness in these layers and before the in-growth of connections from layer 4 (Callaway and Katz, 1992). The clusters also form during binocular deprivation (Callaway and Katz, 1991; Ruthazer and Stryker, 1996). The clusters have been shown to align with the later-forming orientation map in these layers (Callaway and Katz, 1990). They require eye opening in

order to refine, and perhaps to grow to their maximum extent, but this refinement typically consists of increased growth of existing clusters, not a reorganization of them (Callaway and Katz, 1990). This fact is important since it has been shown that the later clusters connect iso-oriented areas (Bosking et al., 1997; Yoshioka et al., 1996). These data imply that the maps in layers 4 and 2/3 are coordinated before they connect to each other. Such coordination would seem to require a different input source. The model proposes that this input is the cortical subplate, and supports this hypothesis with a summary of consistent data and simulations showing that such a mechanism works.

The vertical interlaminar connections are also a key problem for a theory of laminar development. Before eye opening, coarse layer 2/3 clustering makes everything look "coarse." This coarse clustering, however, coexists with precise vertical layer 4-to-2/3 connections. The model proposes how the subplate organizes correlations between layers 4 and 2/3 and thereby guides formation both of coarse horizontal clustering and precise vertical connections between layers.

Models of Map Formation

There is a rich modeling literature on how maps of oriented cells can develop on a cortical sheet. The earliest models demonstrated that a neural network that combines an associative learning rule and recurrent lateral inhibition, or competition, produces orientation tuning when presented with oriented inputs (Grossberg, 1976; von der Malsburg, 1973). Linsker (1986a, 1986b, 1986c) subsequently demonstrated self-organization of orientation tuning without oriented inputs. Other modeling work has shown how ocular dominance maps can arise from uncorrelated inputs (Kohonen, 1982; Miller et al., 1989; Rojer and Schwartz, 1990; Swindale, 1980), how maps of orientation and ocular dominance may develop simultaneously (Durbin and Mitchison, 1990; Obermayer et al., 1992, 1993; Sirosh and Miikkulainen, 1997; Swindale, 1992), and how the development of orientationally tuned simple cells and their arrangement into cortical maps may progress synchronously (Olson and Grossberg 1998, Miller, 1992). While the models vary in their details, Rojer and Schwartz (1990) demonstrated that basic filter properties of lateral excitation and inhibition (i.e. a bandpass filter), naturally produce ocular dominance and orientation columns when they interact with a noise source. Later, Grossberg and Olson (1994) analyzed existent models to show that three common computational principles of all the models lead to familiar map properties: a source of noisy input, a band pass filter, and normalization across all feature dimensions.

More recent modeling work (Grossberg and Raizada, 2000; Grossberg and Williamson, 2001) proposes how laminar circuits in V1 and V2 help to explain data on development, learning, perceptual grouping, and attention. Callaway (1998a) has examined the same substrate anatomically, and has produced a conceptual model in which a layer with horizontal connections (B) receives both the inputs and outputs of a feedforward layer (A), and thus (B) acts as a control system by feeding back to, and modulating the activity of, layer (A).

Subplate Model

The present subplate-cortical developmental model builds on and extends the work of previous models. It demonstrates how the orientation and ocular dominance maps form and are coordinated across multiple area V1 layers. The model also demonstrates the relationship between the development of the orientation map in the input layers and the crude clustering of horizontal connections in the superficial and deep layers.

The model proposes how the subplate circuits embody a source of noisy input, a band pass filter (see Figure 1), and normalization, and thus how orientation and ocular dominance maps develop there. Given the fact that the subplate is involved in the early circuits involving the LGN and the cortical plate, it is natural to assume that the maps learned in the subplate will bias map formation in the other layers. It has been demonstrated that ablation of the subplate results in the lack of formation of orientation selectivity and ocular dominance maps (Ghosh and Shatz, 1992; Kanold et al., 2001). Evolutionary analysis indicates that phylogenic emergence of columns coincides with the emergence of the subplate and, importantly, with the LGN-subplate waiting period (McAllister et al., 1999).

[Insert Figure 2, about here]

One of the model's novel features is that it reflects the temporally ordered process of development. The model starts with a circuit containing the retina, LGN and subplate (Figure 2A). This first circuit is monocular, based upon several lines of evidence. Physiological recordings in area 17 of kittens show that at eye opening the majority of cells respond only to contralateral eye inputs (Albus and Wolf, 1984). Studies in young ferrets demonstrate that the pattern of activity in the LGN is largely unchanged when the ipsilateral inputs from the retina are cut (Welikey and Katz, 1999). In addition, there is an early bias of oriented OFF cells in the kitten cortex (Albus and Wolf, 1984) and of OFF activity in the retina before eye opening (Wong and Oakley, 1996). Correspondingly this stage of the model contains only OFF ganglion cells.

Spontaneous activity in the retina drives the network and correlational learning allows for the development of feedforward and feedback connections between the LGN and subplate. The bandpass properties of the short-range lateral connections in the subplate result in the development of a map of oriented simple cells similar to that found in other models. After development, the pattern of feedforward connections to a given subplate cell and the feedback connections from that cell share the same axis of elongation (Murphy et al., 1999).

The second stage of the model introduces binocular inputs to the subplate (Figure 2B). In this simulation, the connections serving the contralateral eye continue developing as activity in the ipsilateral eye is introduced. The contralateral LGN already has developed oriented connections to the subplate at this stage, whereas those from the ipsilateral LGN are introduced as random spatial receptive fields, just like those of the contralateral LGN before refinement. The spontaneous activity in the retina provides intra-ocular correlations that drive the formation of ocular dominance columns in the subplate.

An important advantage of having ocular dominance columns develop after the orientation map has been specified is that no special mechanisms are needed to coordinate the orientation map between the two eyes. The orientation map of the contralateral eye is inherited by the ipsilateral eye.

Next, the subplate guides map formation in the each of the cortical layers. Because the early map development in each of the cortical layers develops independently (i.e., without interlaminar cortical connections), they are described as separate simulations. This is not meant to imply that the there is no interesting time-course in the map development during this stage. In fact, much of the learning in layer 2/3, which contains much younger cells, occurs after layer 4 has developed its orientation map (Callaway and Katz, 1992; Galuske and Singer, 1996).

In model simulations, the development of layer 4 is next described. In this stage of the model, afferents from the subplate are introduced in layer 4 and the afferents from the LGN begin to develop into layer 4 (Figure 2C). The input from the subplate guides the pattern of developing connections from the LGN into layer 4. The layer 4 circuit includes the same types of mechanisms as the subplate, with the exception that layer 4 also receives input from the subplate in addition to that from the LGN. The input from the subplate biases the development of the LGN inputs to layer

4. Given that the subplate achieves stable learning, it is not surprising that the layer 4 weights stabilize once a map similar to that found in the subplate is achieved. As described in greater detail below, it is assumed that the maps of ocular dominance and orientation tuning form in layer 6 (Figure 2E) at a time similar to that in which they develop in layer 4. The maps in layer 6 develop in the same manner as they do in layer 4.

The model next describes the development of the horizontal connections in layer 2/3 (Figure 2D). Here subplate inputs are introduced to the model layer 2/3. The basis of this circuit *in vivo* are the axonal branches in the marginal zone from the subplate (Ghosh, 1995), where layer 2/3 has dendritic branches (Callaway, 1998b). In this simulation, the connections between layer 2/3 cells develop in response to lateral correlations provided by the subplate inputs. As the connections between layer 2/3 cells develop, the layer 2/3 network amplifies the correlations found in the subplate input and refines the pattern of connections. It is important to realize that the subplate inputs to layer 2/3 are the same as those to layer 4, but in layer 2/3 lateral connections are developed instead of connections from the LGN. While not explicitly modeled, we suggest that the horizontal connections found in layer 5 develop in a similar fashion as those of layer 2/3.

Once maps have developed in each of the cortical layers, interlaminar connections grow (Callaway and Katz, 1992). In the model, layer 4-to-2/3 and layer 6-to-4 connections are developed (Figure 2E). As the subplate provides the same input to each of the cortical layers, there are strong "vertical correlations" in the activity across layers. These correlations, combined with an appropriate correlational learning law, result in cells that have mostly vertical interlaminar connections. These vertical connections are the basis of stable adult columns and are a vital component of the model.

Since the subplate is a transient layer, it is important to show that the cortical circuits and maps are stable after the subplate atrophies. With the introduction of layer 6, the model demonstrates how the circuitry and map structure of the layered cortical circuit can be maintained. The model layer 6 receives inputs from the subplate and develops a similar pattern of connections from the LGN as is found from the LGN to layer 4. Layer 6 also develops a set of connections to the LGN, which are similar to those from the subplate to the LGN. As noted above, interlaminar connections from layer 6 to layer 4 are developed. When the layer 6 connections have stabilized, the subplate is removed from the network and simulations demonstrate that this new, adult-like, circuit is stable.

Finally, patterned vision is used to allow for the formation of distinct ON and OFF subregions of simple cell receptive fields. While the earlier orientationally tuned cells found in cortex are monocular and are mostly dominated by OFF inputs, mature cells contain both ON and OFF subregions. The model accomplishes this in a simulation of eye opening. At eye opening, the mean firing rates of the ON and OFF cells in the retina equalizes. More importantly, with the introduction of patterned vision, the ON and OFF cells in the retina become anti-correlated: wherever an ON cell is active, the OFF cell at that location is hyperpolarized and a spatially neighboring OFF cell is active. *In vivo*, layer 4 cells quickly develop distinct ON and OFF subfields (see Albus and Wolf, 1984).

Ablation of the subplate, shortly after afferents from the LGN contact layer 4, results in a loss of orientation tuning and ocular dominance column development in layer 4. It has been demonstrated that the levels of brain-derived neurotrophic factor (BDNF) increase dramatically at this time (Ghosh and Shatz, 1994). Other data demonstrate that either an increase or decrease of the intrinsic level of BDNF in cortex will result in the loss of ocular dominance columns (Cabelli et al., 1995, 1997). BDNF has been shown to increase the release of both Glutamate and GABA (Berardi and Maffei, 1999).

To model the effects of subplate ablation, the subplate layer is removed from the network and random weights are introduced between the LGN and layer 4. In addition, a parameter is introduced to the activity equation for layer 4 that equally modulates the effectiveness of the excitatory and inhibitory connections. To model the effects of an increase of BDNF, this term is increased. To model a reduction of BDNF, this term is reduced. A sufficiently large change in either direction interferes with the development of orientation tuning and ocular dominance columns.

Model Equations

The model equations are chosen to be consistent with those used in the FACADE model (Grossberg, 1994, 1997; Grossberg and Mcloughlin 1997; Grossberg et al., 2002) of 3-D vision and figure-ground perception. Earlier modeling of visual development within this framework has illustrated how development can lead to an adult model that can simulate data about adult human psychophysics (Grossberg and Williamson, 2001). The present modeling results are consistent with these demonstrations and extend them to analyze the coordinating role of the subplate in cortical development.

The symbols and notation used in the network equations are as follows. Superscripts abbreviate each area of the model: (R) for Retina, (L) for LGN, (S) for Subplate and (3), (4), (6) for layers 2/3, 4, and 6, respectively. Subscripts denote the position of a cell in each area: i and j, denote horizontal and vertical spatial coordinates, and l denotes which of the four regions in the two eyes to which a cell belongs: Contra-ON, Contra-OFF, Ipsi-ON, and Ipsi-OFF. For example, $I_{ijl}^{(R)}$ is an input to a retinal cell, and, $x_{ij}^{(S)}$ is the activity of a subplate cell. Note that l does not appear in the subplate input, or anywhere in the cortex, since the inputs from all retinal regions converge onto each cortical layer.

The model was implemented in the Matlab simulation environment and run on a dual 1.4 Ghz Athalon computer running Linux. In the retina, activity was assumed to react quickly to noise fluctuations and was thus computed at steady state. The other continuous time cell activity equations were solved using an adaptive step size Runge-Kutte 4,5 method. For computational simplicity, the equations for learning by the adaptive weights were solved at a slower time scale using Euler's method. Each stage of the model was run for 20,000-100,000 input iterations until the weights converged to a stable pattern.

Retina

Retinal inputs, $I_{ijl}^{(R)}$, to the model are based upon data about spontaneous activity in the retina. $I_{ijl}^{(R)}$ is generated by thresholding a set of random numbers chosen from a normal distribution, which allows 5-10% of cells to be active at a given time, consistent with estimates of the rate of spontaneous activity found in the LGN (Papaioannou and White, 1972; Kaplan et al., 1987). Successful simulations have also been run using white noise.

For simulations mimicking patterned vision after eye opening, we modeled the structured visual inputs with randomly sized, positioned and oriented rectangles, as described in Grossberg and Williamson (2001). This is in keeping with the idea that essentially all visual objects have linear contours on a sufficiently small spatial scale. Each input contained seven rectangles, each with a luminance that was randomly distributed between 0 and 2. The length and width of each rectangle was determined by an iterative random process in which each dimension started at zero

pixels, grew (independently) by one pixel at each iteration, and stopped growing with probability .1 at each iteration. The images were processed with wrap-around in both the x and y dimensions to avoid spurious boundary effects.

Retinal activity, $x_{ij}^{(R)}$, is assumed to obey a membrane, or shunting, equation whose inputs result from putting $I_{ijl}^{(R)}$ through an on-center/off-surround (see Figure 1) feedforward network:

$$\frac{dx_{ijl}^{(R)}}{dt} = -A^{(R)}x_{ijl}^{(R)} + \left(B^{(R)} - x_{ijl}^{(R)}\right)\sum_{uv} G_{ijuv}^{(R+)}I_{uvl}^{(R)} - \left(C^{(R)} + x_{ijl}^{(R)}\right)\sum_{uv} G_{ijuv}^{(R-)}I_{uvl}^{(R)} \quad . \tag{1}$$

Such a membrane, or shunting equation, captures key properties of the activity of neurons (Grossberg, 1973; Hodgkin and Huxley, 1952). Here, $A^{(R)}$ represents the leakage coefficient and $B^{(R)}$ and $C^{(R)}$ represent the excitatory and inhibitory reversal potentials, respectively. The terms $G_{uvij}^{(R+)}$ and $G_{uvij}^{(R-)}$ represent the on-center and off-surround receptive fields, respectively, and are defined by a two-dimensional normalized Gaussian kernel:

$$G_{ijuv}^{(R+/-)} = \frac{1}{2\pi\left(\sigma^{(R+/-)}\right)^2} e^{\frac{-(u-i)^2-(v-j)^2}{2\sigma^{(R+/-)^2}}} \quad . \tag{2}$$

Parameters for the Retina are $A^{(R)} = 1$, $B^{(R)} = 5$, $C^{(R)} = 5$, $\sigma^{(R+)} = \frac{1}{\sqrt{2}}$, and $\sigma^{(R-)} = \frac{3}{\sqrt{2}}$.

Lateral Geniculate Nucleus

The outputs from the retina are thresholded functions of retinal activity, namely $\left[x_{ijl}^{(R)}\right]^+ = \max\left(x_{ijl}^{(R)}, 0\right)$. These outputs are fed into a model of the LGN via a feedforward on-center/off-surround network. The LGN activity, $x_{ijl}^{(L)}$, is also modulated multiplicatively by feedback, $I_{ijl}^{(L)}$, from the subplate:

$$\begin{aligned}\frac{dx_{ijl}^{(L)}}{dt} = -A^{(L)}x_{ijl}^{(L)} &+ (B^{(L)} - x_{ijl}^{(L)})\sum_{uv}\left[G_{ijuv}^{(L+)}\left(D^{(L)}I_{uvl}^{(L)} + 1\right)[x_{uvl}^{(R)}]^+\right] \\ &-(C^{(L)} + x_{ijl}^{(L)})\sum_{uv}\left[G_{ijuv}^{(L-)}\left(E^{(L)}I_{uvl}^{(L)} + 1\right)[x_{uvl}^{(R)}]^+\right]\end{aligned} \quad . \tag{3}$$

The subplate feedback signals are defined by:

$$I_{ijl}^{(L)} = \sum_{uv} F\left(x_{uv}^{(S)}\right)w_{uvijl}^{(SL)} \quad . \tag{4}$$

Here $F\left(x_{uv}^{(S)}\right)$ represents a sigmoid output signal function of subplate activity:

$$F\left(x^{(S)}\right) = \frac{T\left(x^{(S)}\right)^n}{T\left(x^{(S)}\right)^n + f^n}, \tag{5}$$

The parameters n and f are fixed for all layers, and,

$$T\left(x^{(S)}\right) = \begin{cases} x^{(S)} & \text{if } x^{(S)} \geq \Gamma^{(S)} \\ 0 & \text{otherwise} \end{cases} \quad . \tag{6}$$

In this equation, the parameter Γ follows the superscript of the input. For example, in $T\left(x^{(L)}\right)$ the threshold $\Gamma^{(L)}$ is used instead of $\Gamma^{(S)}$.

In the model, the outputs of LGN cells are threshold-linear, as in (6), due to the linear properties of LGN X cells, whereas the cortical outputs are represented by sigmoid signal functions (Sclar et al., 1985; Skottun et al., 1987; Maunsell et al., 1999), as in (5).

The top-down adaptive weights, $w_{uvijl}^{(SL)}$, from subplate position (u,v) to LGN position (i,j,l) in (4) are learned adaptively, using an outstar learning law (Grossberg 1968, 1980):

$$\frac{dw_{uvijl}^{(SL)}}{dt} = A^{(SL)} F\left(x_{uv}^{(S)}\right)\left[T\left(x_{ijl}^{(L)}\right) - w_{uvijl}^{(L)}\right]. \tag{7}$$

In this associative learning law, learning is gated on or off by the activity of a presynaptic signal, in this case a top-down output signal from the subplate, $F\left(x_{uv}^{(S)}\right)$; see (5). The weights track the threshold level of activity in the LGN, $T\left(x_{ijl}^{(L)}\right)$; see (6). An outstar law is often used to learn a pattern of activity via feedback connections at sampled cells, whereas an instar learning law (see below for definition) is invoked for feedforward connections (Carpenter and Grossberg, 1987). Parameters for the LGN equations are: $A^{(L)} = 1$, $B^{(L)} = 5$, $C^{(L)} = 5$, $D^{(L)} = 10$, $E^{(L)} = 10$, $\sigma^{(L+)} = \frac{1}{\sqrt{2}}$, $\sigma^{(L-)} = \frac{3}{\sqrt{2}}$, $A^{(SL)} = 0.25$, $\Gamma^{(S)} = 0.001$, $n = 3$, $f = 0.8$, and $\Gamma^{(L)} = 0.3$.

Subplate

The output of the LGN is fed into a model of the cortical subplate. The activity of the subplate, $x_{ij}^{(S)}$, is defined via a combination of feedforward and feedback on-center/off-surround interactions:

$$\begin{aligned}\frac{dx_{ij}^{(S)}}{dt} = -A^{(S)} x_{ij}^{(S)} + (B^{(S)} - x_{ij}^{(S)}) \sum_{uv} G_{ijuv}^{(S+)} z_{uv}^{(S)} \left[I_{uv}^{(S)} + D^{(S)}\left(F\left(x_{uv}^{(S)}\right) + F\left(x_{uv}^{(4)}\right)\right)\right] \\ -(C^{(S)} + x_{ij}^{(S)}) \sum_{uv} G_{ijuv}^{(S-)} \left[I_{uv}^{(S)} + E^{(S)}\left(F\left(x_{uv}^{(S)}\right) + F\left(x_{uv}^{(4)}\right)\right)\right]\end{aligned}. \tag{8}$$

The input, $I_{ij}^{(S)}$, to the subplate from the LGN is computed by gating bottom-up LGN signals, $T\left(x_{uvl}^{(L)}\right)$, with adaptive weights, $w_{uvlij}^{(LS)}$, before summing them across all LGN cell positions (u,v) and layers l (ON, OFF, contralateral, ipsilateral):

$$I_{ij}^{(S)} = \sum_{uvl} T\left(x_{uvl}^{(L)}\right) w_{uvlij}^{(LS)}. \tag{9}$$

A notable difference between the subplate and the LGN is the presence of horizontal positive and negative feedback, $F\left(x_{uv}^{(S)}\right)$, consistent with data showing isotropic excitatory and inhibitory anatomical connections in the subplate (Galuske and Singer, 1996). In later occurring simulations, where layer 4 is present, feedback from layer 4, $F\left(x_{uv}^{(4)}\right)$, also influences the subplate (Callaway 1998b; Ghosh, 1995). Feedback from layer 4 to the subplate is additive, unlike the multiplicative feedback from the subplate to the LGN, and thus acts as an additional input to the subplate, rather than as the gain control found in the LGN.

Another trait of the subplate is the presence of habituative, or depressing, synaptic transmitters, $z_{ij}^{(S)}$ (Abbott et al., 1997; Grossberg 1976, 1980; Markram and Tsodyks, 1996). Habituative transmitters prevent the earliest cells that learn from persistently dominating network dynamics:

$$\frac{dz_{ij}^{(S)}}{dt} = A^{(Sz)}(1 - z_{ij}^{(S)}) - B^{(Sz)} z_{ij}^{(S)} \left[I_{ij}^{(S)} + D^{(S)} \left(F\left(x_{ij}^{(S)}\right) + F\left(x_{ij}^{(4)}\right) \right) \right]^2. \tag{10}$$

The habituative transmitters, $z_{ij}^{(S)}$, vary between the value of 1 and zero. When $z_{ij}^{(S)} = 1$, the synapse is at full strength, and at values less than 1 the level of the transmitter is diminished. The parameter $A^{(Sz)}$ governs the rate of recovery of the transmitter, whereas the parameter $B^{(Sz)}$ governs the rate of habituation. Habituation occurs at a rate proportional to the square of the amplitude of the inputs that the transmitter gates in (8), namely $\left[I_{ij}^{(S)} + D^{(S)} \left(F\left(x_{ij}^{(S)}\right) + F\left(x_{ij}^{(4)}\right) \right) \right]^2$. The squaring of this input allows for proportionately greater habituation for large inputs than small (Gaudiano and Grossberg, 1991).

The bottom-up adaptive weights, $w_{uvlij}^{(LS)}$, from LGN position (u,v,l) to subplate position (i,j), are computed by an instar learning law that conserves the total weight converging onto each subplate cell (Carpenter and Grossberg, 1987; Grossberg, 1976, 1980):

$$\frac{dw_{uvlij}^{(LS)}}{dt} = A^{(LS)} F\left(x_{ij}^{(S)}\right) \left[T\left(x_{uvl}^{(L)}\right) \left(B^{(LS)} - \sum_{pqr} w_{pqrij}^{(LS)} \right) - w_{uvlij}^{(LS)} \sum_{pqr \neq uvl} T\left(x_{pqr}^{(L)}\right) \right]. \tag{11}$$

The instar is postsynaptically gated by the subplate signal $F\left(x_{ij}^{(S)}\right)$, and, unlike the outstar, the weights track the level of the bottom-up signal from the LGN, $T\left(x_{uvl}^{(L)}\right)$; see (6). The parameter $B^{(LS)}$ limits the total weight to a given subplate cell, and is consistent with evidence for limited neurotrophic factors (Purves, 1988). In the model, conservation plays a role in the formation of ocular dominance columns, and in simulations lacking conservation, the ipsilateral eye fails to take over territory in the subplate since the weights from the contralateral eye are already large. This effect is similar to that obtained in models that place explicit limits on the levels of trophic factors (Elliot and Shadbolt, 1999).

The spatial extent of LGN inputs to each subplate cell is limited to a circular region for computational efficiency. Thus (11) holds if $u^2 + v^2 \leq 16$; otherwise, $w_{uvlij}^{(LS)} = 0$. Simulations have been run to demonstrate that extending this limit does not lead to qualitatively different results. Parameters for the subplate equations are: $A^{(S)} = 1$, $B^{(S)} = 6$, $C^{(S)} = 6$, $D^{(S)} = 20$, $E^{(S)} = 20$, $\sigma^{(S+)} = \frac{3}{4\sqrt{2}}$, $\sigma^{(S-)} = \frac{3}{\sqrt{2}}$, $\Gamma^{(4)} = 0.001$, $A^{(Sz)} = 0.5$, $B^{(Sz)} = 5$, $A^{(LS)} = 0.25$, and $B^{(LS)} = 5$.

Layer 4

The activity of layer 4, $x_{ij}^{(4)}$, obeys an equation similar to (8) for the subplate:

$$\begin{aligned} \frac{dx_{ij}^{(4)}}{dt} = -A^{(4)} x_{ij}^{(4)} &+ (B^{(4)} - x_{ij}^{(4)}) \sum_{uv} G_{ijuv}^{(4+)} z_{uv}^{(4)} J^{(4)} \left[I_{uv}^{(4)} + D^{(4)} \left(F\left(x_{uv}^{(S)}\right) + F\left(x_{uv}^{(4)}\right) \right) \right] \\ &- (C^{(4)} + x_{ij}^{(4)}) \sum_{uv} G_{ijuv}^{(4-)} J^{(4)} \left[I_{uv}^{(4)} + E^{(4)} \left(F\left(x_{uv}^{(S)}\right) + F\left(x_{uv}^{(4)}\right) \right) \right] \end{aligned}. \tag{12}$$

The habituative transmitters, $z_{ij}^{(4)}$, prevent the earliest cells that learn from persistently dominating network dynamics:

$$\frac{dz_{ij}^{(4)}}{dt} = A^{(4z)} \left(1 - z_{ij}^{(4)}\right) - B^{(4z)} z_{ij}^{(4)} \left[I_{ij}^{(4)} + D^{(4)} \left(F\left(x_{ij}^{(S)}\right) + F\left(x_{ij}^{(4)}\right) \right) \right]^2. \tag{13}$$

The modulatory term, $J^{(4)}$, models the effect of changing BDNF levels. Varying the value of $J^{(4)}$ allows us to approximate an equal percent change of release of GABA and Glutamate (Berardi and Maffei, 1999). Unless otherwise mentioned, $J^{(4)}$ is set to 1.

The input, $I_{ij}^{(4)}$, to layer 4 from the LGN is computed by gating bottom-up LGN signals, $T\left(x_{uvl}^{(L)}\right)$, with adaptive weights, $w_{uvlij}^{(L4)}$, before summing them across all LGN cell positions (u,v) and layers l (ON, OFF, contralateral, ipsilateral):

$$I_{ij}^{(4)} = \sum_{uvl} T\left(x_{uvl}^{(L)}\right) w_{uvlij}^{(L4)} \ . \tag{14}$$

The bottom-up adaptive weights, $w_{uvlij}^{(L4)}$, from LGN position (u,v,l) to layer 4 position (i,j), are computed by an instar learning law, which conserves the total weight converging onto each layer 4 cell:

$$\frac{dw_{uvlij}^{(L4)}}{dt} = A^{(L4)} F\left(x_{ij}^{(4)}\right)\left[T\left(x_{uvl}^{(L)}\right)\left(B^{(L4)} - \sum_{pqr} w_{pqrij}^{(L4)}\right) - w_{uvlij}^{(L4)} \sum_{pqr \neq uvl} T\left(x_{pqr}^{(L)}\right)\right]. \tag{15}$$

The spatial extent of LGN inputs to each layer 4 cell is limited to a circular region for computational efficiency. Thus (15) holds if $u^2 + v^2 \leq 16$; otherwise, $w_{uvlij}^{(L4)} = 0$.

The LGN-to-4 weights, $w_{uvlij}^{(L4)}$, start with values of zero. Early in the simulation, these weights are small, and the inputs from the subplate dominate the activity of layer 4 cells. This allows the subplate to instruct the pattern of weights in layer 4, which are stabilized by the same circuit mechanisms in layer 4 that allows the weights from the LGN to the subplate to stabilize. The assumption of zero initial weights is not necessary, as simulations beginning with random LGN-to-layer 4 weights also successfully learn the subplate maps. Parameters for the layer 4 equations are: $A^{(4)} = 1$, $B^{(4)} = 6$, $C^{(4)} = 6$, $D^{(4)} = 30$, $E^{(4)} = 30$, $\sigma^{(4+)} = \frac{3}{4\sqrt{2}}$, $\sigma^{(4-)} = \frac{3}{\sqrt{2}}$, $A^{(4z)} = 0.5$, $B^{(4z)} = 5$, $A^{(L4)} = 0.25$, and $B^{(L4)} = 5$.

Layer 2/3 Long-Range Connection Development

The activity of layer 2/3, $x_{ij}^{(3)}$, obeys an equation similar to that of the other layers except that adaptive horizontal connections also exist:

$$\begin{aligned}\frac{dx_{ij}^{(3)}}{dt} = -A^{(3)} x_{ij}^{(3)} &+ (B^{(3)} - x_{ij}^{(3)}) \sum_{uv} G_{ijuv}^{(3+)}\left[z_{uv}^{(3)} I_{uv}^{(3)} + D^{(3)} F\left(x_{uv}^{(S)}\right)\right] \\ &-(C^{(3)} + x_{ij}^{(3)}) \sum_{uv} G_{ijuv}^{(3-)}\left[I_{uv}^{(3)} + E^{(3)} F\left(x_{uv}^{(S)}\right)\right]\end{aligned} \ . \tag{16}$$

The habituative transmitters, $z_{ij}^{(3)}$, prevent the earliest cells that learn from persistently dominating network dynamics. Here these transmitters gate the horizontal connections:

$$\frac{dz_{ij}^{(3)}}{dt} = A^{(3z)}(1 - z_{ij}^{(3)}) - B^{(3z)} z_{ij}^{(3)}\left(I_{ij}^{(3)}\right)^2. \tag{17}$$

The input, $I_{ij}^{(3)}$, to each layer 2/3 cell from other layer 2/3 cells is:

$$I_{ij}^{(3)} = \sum_{uv} F\left(x_{uv}^{(3)}\right) w_{uvij}^{(3)} . \tag{18}$$

An instar learning law is used to compute the adaptive weights, $w_{uvij}^{(3)}$, between layer 2/3 cells:

$$\frac{dw_{uvij}^{(3)}}{dt} = A^{(3w)} F\left(x_{ij}^{(3)}\right)\left[F\left(x_{uv}^{(3)}\right) - w_{uvij}^{(3)}\right]. \tag{19}$$

The spatial extent of horizontal connections in layer 2/3 is limited for computational efficiency. Thus (19) holds if $u^2 + v^2 \le 144$; otherwise, $w_{uvij}^{(3)} = 0$.

In layer 2/3, the only feedforward source of input, $F\left(x_{uv}^{(S)}\right)$, is from the subplate. The lateral weights, $w_{uvij}^{(3)}$, start with values of zero and the correlations in the input from the subplate guide the outgrowth of connections layer 2/3 connections. As these connections develop, recurrent bursts of activity become common in this layer, as found *in vivo* (Welikey and Katz, 1999). Parameters for the layer 2/3 equations are: $A^{(3)} = 1$, $B^{(3)} = 10$, $C^{(3)} = 10$, $D^{(3)} = 10$, $E^{(3)} = 10$, $\sigma^{(3+)} = \sqrt{2}$, $\sigma^{(3-)} = 2\sqrt{2}$, $\Gamma^{(3)} = 0.01$, $A^{(3z)} = 0.05$, $B^{(3z)} = 0.5$, and $A^{(3w)} = 0.01$.

Layer 6

The activity of layer 6, $x_{ij}^{(6)}$, obeys an equation similar to that of layer 4:

$$\begin{aligned}\frac{dx_{ij}^{(6)}}{dt} = -A^{(6)} x_{ij}^{(6)} &+ (B^{(6)} - x_{ij}^{(6)}) \sum_{uv} G_{ijuv}^{(6+)} z_{uv}^{(6)} \left[I_{uv}^{(6)} + D^{(6)}\left(F\left(x_{uv}^{(S)}\right) + F\left(x_{uv}^{(6)}\right)\right)\right] \\ &-(C^{(6)} + x_{ij}^{(6)}) \sum_{uv} G_{ijuv}^{(6-)} \left[I_{uv}^{(6)} + E^{(6)}\left(F\left(x_{uv}^{(S)}\right) + F\left(x_{uv}^{(6)}\right)\right)\right]\end{aligned}. \tag{20}$$

The habituative transmitters, $z_{ij}^{(6)}$, prevent the earliest cells that learn from persistently dominating network dynamics:

$$\frac{dz_{ij}^{(6)}}{dt} = A^{(6z)}\left(1 - z_{ij}^{(6)}\right) - B^{(6z)} z_{ij}^{(6)} \left[I_{ij}^{(6)} + D^{(6)}\left(F\left(x_{ij}^{(6)}\right) + F\left(x_{ij}^{(S)}\right)\right)\right]^2. \tag{21}$$

The input, $I_{ij}^{(6)}$, to layer 6 from the LGN is computed by gating bottom-up LGN signals, $T\left(x_{uvl}^{(L)}\right)$, with adaptive weights, $w_{uvlij}^{(L6)}$, before summing them across all LGN cell positions (u,v) and layers l (ON, OFF, contralateral, ipsilateral):

$$I_{ij}^{(6)} = \sum_{uvl} T\left(x_{uvl}^{(L)}\right) w_{uvlij}^{(L6)}. \tag{22}$$

The bottom-up adaptive weights, $w_{uvlij}^{(L6)}$, from the LGN to layer 6 are computed by an instar learning law, which conserves the total output from each LGN cell:

$$\frac{dw_{uvlij}^{(L6)}}{dt} = A^{(L6)} F\left(x_{ij}^{(6)}\right)\left[T\left(x_{uvl}^{(L)}\right)\left(B^{(L6)} - \sum_{pqr} w_{pqrij}^{(L6)}\right) - w_{uvlij}^{(L6)} \sum_{pqr \ne uvl} T\left(x_{pqr}^{(L)}\right)\right]. \tag{23}$$

The spatial extent of LGN inputs to each layer 6 cell is limited to a circular region for computational efficiency. Thus (23) holds if $u^2 + v^2 \le 16$; otherwise, $w_{uvlij}^{(L6)} = 0$.

Top-down adaptive weights, $w_{uvijl}^{(6L)}$, from layer 6 to the LGN are learned using an outstar learning law:

$$\frac{dw_{uvijl}^{(6L)}}{dt} = A^{(6L)} F\left(x_{uv}^{(6)}\right)\left[T\left(x_{ijl}^{(L)}\right) - w_{uvijl}^{(6L)}\right]. \tag{24}$$

Parameters for the layer 6 equations are: $A^{(6)}=1$, $B^{(6)}=6$, $C^{(6)}=6$, $D^{(6)}=30$, $E^{(6)}=30$, $\sigma^{(6+)}=\frac{3}{4\sqrt{2}}$, $\sigma^{(6-)}=\frac{3}{\sqrt{2}}$, $\Gamma^{(6)}=0.001$, $A^{(6z)}=0.5$, $B^{(6z)}=5$, $A^{(L6)}=0.25$, $B^{(L6)}=5$, and $A^{(6L)}=0.25$.

Development of Interlaminar Connections

Interlaminar connections from layer 4-to-2/3, $w_{uvij}^{(43)}$, and from layer 6-to-4, $w_{uvij}^{(64)}$, are developed in the final set of simulations. The layer 6-to-4 weights, $w_{uvij}^{(64)}$, are computed by an instar learning law:

$$\frac{dw_{uvij}^{(64)}}{dt}=A^{(64)}F\left(x_{ij}^{(4)}\right)\left[F\left(x_{uv}^{(6)}\right)-w_{uvij}^{(64)}\right]. \tag{25}$$

The layer 4-to-2/3 weights, $w_{uvij}^{(43)}$, are also computed by an instar learning law:

$$\frac{dw_{uvij}^{(43)}}{dt}=A^{(43)}F\left(x_{ij}^{(3)}\right)\left[F\left(x_{uv}^{(4)}\right)-w_{uvij}^{(43)}\right]. \tag{26}$$

These simulations are run in two stages. First, the interlaminar connections are developed guided by the subplate activity. For these simulations, $\left(F\left(x_{uv}^{(6)}\right)w_{ijuv}^{(6L)}+F\left(x_{uv}^{(S)}\right)w_{ijuv}^{(SL)}\right)$ replaces $F\left(x_{uv}^{(S)}\right)w_{ijuv}^{(SL)}$ in (4), $\left(F\left(x_{uv}^{(S)}\right)+\sum_{uv}F\left(x_{uv}^{(6)}\right)w_{uvij}^{(64)}\right)$ replaces $F\left(x_{uv}^{(S)}\right)$ in (12) and (13), and $\left(F\left(x_{uv}^{(S)}\right)+\sum_{uv}F\left(x_{uv}^{(3)}\right)w_{uvij}^{(43)}\right)$ replaces $F\left(x_{uv}^{(S)}\right)$ in (16). Once the interlaminar connections partially develop, the model subplate is removed and simulations demonstrate that the network remains stable. Explicitly, $F\left(x_{uv}^{(S)}\right)w_{ijuv}^{(SL)}$ is removed from (4), $F\left(x_{uv}^{(S)}\right)$ is removed from (12) and (13), and $F\left(x_{uv}^{(S)}\right)$ is removed from (16). Parameters are: $A^{(43)}=0.01$ and $A^{(64)}=0.01$.

Results

Development of Orientation in the Subplate

The model starts with a circuit containing the retina, LGN and subplate (Figure 2A). This model is similar to other models of how orientation maps develop and it produces a robust map of oriented cells; see Figure 3A. This figure shows a 9-by-9 region in the center of the network and was constructed by probing the network bars of 8 different orientations and measuring the peak response of each cell to each orientation. The orientation of each bar portrays the orientation of the stimulus that elicited the maximum response from that cell. The length of each bar portrays the orientation index of that cell (the difference between the peak and null (stimulus orthogonal to the peak) orientations divided by their sum). Using vector sums to determine the peak and circular variance as an index produce similar maps. Figure 3 also shows the raw receptive fields (Figure 3B) for 4 neighboring cells in the middle of the network, their orientation tuning curves (Figure 3C), and the schematic of their orientation tuning (Figure 3D).

[Insert Figure 3, about here]

The receptive fields in this model are spatially defined and thus there is great diversity in the degree of tuning and the shape of the raw receptive fields, shown in Figure 4. Feedback connections from the subplate to LGN are developed simultaneously to the development of the feedforward LGN-to-subplate connections. After development, the feedforward connections to a given subplate cell and the feedback connections from that cell share the same long-axis (c.f., Murphy et al., 1999). This figure shows the receptive fields before and after learning. Initial weight profiles from the LGN to subplate are generated as white spatial noise with limited spatial extent (Figure 4A). After learning, weights from the LGN to subplate are refined and oriented (Figure 4C). Initial weight profiles from the subplate to LGN are initially uniform and equal to 1 (Figure 4B). After learning weights from subplate to LGN are also patterned and are oriented in the same manner as their equivalent LGN to subplate weights (Figure 4D).

[Insert Figure 4, about here]

Development of Ocular Dominance in the Subplate

The second stage of the model introduces binocular inputs in the subplate (Figure 2B). In this simulation, ocular dominance columns emerge, as in Figure 5. Plotted is the ocularity index (the difference of the ipsilateral and contralateral weights divided by the sum). This index is valued between –1 and 1, where cells with large absolute values are the most monocular. In this simulation, the typical cell has an index of +/- .8 which means that they are highly monocular. At the beginning of the simulation, the cells are all dominated by the contralateral eye. The ipsilateral eye invades territory that was only weakly activated by the contralateral eye. Since the total connection strength to each subplate cell is conserved, competition results in cells that are largely monocular. Since the total input from each eye to the subplate is equal, the number of cells devoted to each eye equalizes (Miller et al., 1989). Finally, the width of the columns approximates the extent of the local excitatory and inhibitory connections (c.f., Fitzpatrick et al., 1985; Lund et al., 1995).

[Insert Figure 5, about here]

Layer 4 simulations

In this simulation, afferents from the subplate are introduced in layer 4 and the afferents from the LGN begin to grow into layer 4 (Figure 2C). The layer 4 simulations demonstrate that the orientation and ocular dominance maps, which are learned in the subplate, can be subsequently taught to other cortical layers, as shown in Figure 6. Here it can be seen the orientation and ocular dominance maps are almost identical between the two layers. A comparison of the peak orientations between the subplate and layer 4 shows that 80% of the layer 4 cells have the same orientation peak as is found in the underlying subplate cell. A comparison of the receptive fields between the subplate and layer 4 shows that, in almost every case, pattern weights from the LGN to layer 4 correspond to those from the LGN to the subplate. There is a 96% correlation between these weights in a pixel-by-pixel comparison.

[Insert Figure 6, about here]

Subplate Ablation and BDNF

Ablation of the subplate results in a loss of orientation tuning and ocular dominance column development in layer 4. It has been demonstrated that the levels of brain-derived neurotrophic factor

(BDNF) increase dramatically at this time (Ghosh and Shatz, 1994). Other data demonstrate that either an increase or decrease of the intrinsic level of BDNF in cortex will result in the loss of ocular dominance columns (Cabelli et al., 1995, 1997). BDNF has been shown to increase the release of both Glutamate and GABA (Berardi and Maffei, 1999).

[Insert Figure 7, about here]

To model the effects of subplate ablation, the subplate inputs were removed from layer 4 and the LGN. In addition, parameter $J^{(4)}$ is introduced to activity equation (12) that describes layer 4. To model the effects of an increase of BDNF, $J^{(4)}$ is increased. As shown in Figure 7, if $J^{(4)} \geq 1.5$, the initial pattern of weights from the LGN to layer 4, which were initialized to random values, failed to refine. Thus neither ocular dominance columns nor orientation develop in layer 4. If $J^{(4)} = 1$ (i.e., baseline BDNF), ocular dominance and orientation maps will form normally, but will have no relationship to the maps that existed in the subplate before it was ablated. If $J^{(4)} \leq 5$, receptive fields do refine, but are not well oriented and ocular dominance does not develop. In addition, the receptive fields that develop with low values of $J^{(4)}$ are not stable; see Figure 8.

[Insert Figure 8, about here]

We have shown that an equal change to both excitation and inhibition will affect map development. A sufficiently large increase of the net level of excitation or inhibition will also interfere with the development of ocular dominance columns and orientation tuning. An increase of excitation reduces the selectivity of cells by enlarging their receptive fields. An increase of inhibition, beyond a certain point, causes a loss of cell response and thus more random receptive fields.

An alternate explanation of the role of BDNF is that LGN neurons require BDNF to survive. In cases where BDNF is abundant, the LGN neurons proliferate. Where BDNF is scarce, the LGN inputs atrophy. In this situation, only a certain range of BDNF levels will produce the necessary competition for resources that produce ocular dominance columns.

Development of ON/OFF receptive fields

While the early orientationally tuned cells found in cortex are dominated by OFF inputs, mature cells contain both ON and OFF subregions; see Figure 2C. The model accomplishes this in a simulation of developmental dynamics around the time of eye opening. At eye opening, the mean firing rates of the ON and OFF cells in the retina equalizes. More importantly, with the introduction of patterned vision, the ON and OFF cells in the retina become anti-correlated: wherever an ON cell is active, the OFF cell at that location is hyperpolarized and a spatially neighboring OFF cell is active. *In vivo*, layer 4 cells quickly develop distinct ON and OFF subfields (see Albus and Wolf, 1984).

[Insert Figure 9, about here]

The model uses an input consisting of patterns of randomly configured rectangles, of random luminance and orientation, as described in Grossberg and Williamson (2001). Filtering such an image separately with ON or OFF filters produces patterns that have spatially offset areas of high activation. In the network, the OFF cell activities are spatially offset from those of the ON cells and, as a result, correlational learning in layer 4 produces cells with distinct ON and OFF subfields; see Figure 9.

Layer 2/3 simulations

In this simulation, the subplate instructs the growth of intralaminar connections in layer 2/3, as in Figure 2D. Results from this simulation are shown in Figure 10A. Each block represents the lateral connections from a single layer 2/3 cell. Connections of strong weight, in white, are clustered together separated by gaps, in black, of zero or small weight. Here the pattern of horizontal connections is more refined than the scattered horizontal connections found *in vivo* (Callaway and Katz, 1990). We suggest that this qualitative difference results from the fact that there is no noise in the Difference-of-Gaussian filters used in the simulation (see Figure 1). In the model, the size of the clusters is determined by the extent of the local excitatory interactions, whereas the spacing between the clusters is influenced by the extent the local inhibitory connections. If these filters were multiplied with noise, the clustered horizontal connections would be more scattered as found *in vivo*.

In the current simulations, the clusters correspond to underlying subplate cells of all orientations. We predict that the early clusters found before eye opening *in vivo* are also nonspecific to orientation. This is consistent with the double-label data from Callaway and Katz (1990), where they applied a retrograde stain in the same area of the same animal at both P15 and P29. These data show that the P29 stain labels areas that were stained with the P15 tracer, but also that the P15 stain labels many areas that are no longer labeled at P29. It seems that during the refinement of the clusters, which occurs when the eyes are opened, that connections to ortho-orientations drop off, resulting in horizontal connections to iso-oriented regions of the orientation map (Bosking et al., 1997).

[Insert Figure 10, about here]

Development of Layer 4 to Layer 2/3 Connections

After clusters form in layer 2/3, connections from layer 4 to layer 2/3 are developed; see Figure 2E. The formation of a map in the subplate and connections of the subplate with other cortical layers provides the "vertical correlations" that are necessary for proper interlaminar connections, which support cortical columns, to form.

The results of this simulation are shown in Figure 10B. In this figure, the white spots in the center of each block demonstrate that cells in layer 4 are connected to the directly overlying layer 2/3 cells. Together, the simulations in Figure 10 show how coarsely clustered intralaminar connections in layer 2/3 can coexist with precisely organized vertical interlaminar connections.

Death of The Subplate (the rise of layer 6)

Since the subplate is a transient layer, it is important to show that the cortical circuits and maps are stable after the subplate atrophies. With the introduction of layer 6, the model demonstrates how the circuitry and map structure of the layered cortical circuit can be maintained; see Figure 2E.

[Insert Figure 11, about here]

The results of the layer 6 simulations are summarized in Figure 11. Layer 6 has inputs from the subplate and it develops a nearly identical pattern of connections from the LGN as is found from the LGN to layer 4; compare Figures 11A and 11C with Figures 11B and 11D. Here there is a 93%

correlation in a pixel-by-pixel comparison. Layer 6 develops a set of connections to the LGN, which are similar to those from the subplate to the LGN, with a 96% correlation.

In addition, interlaminar connections from layer 6 to layer 4 are developed; see Figure 12A. These interlaminar connections develop vertically in a similar fashion as the layer 4 to layer 2/3 connections. When all sets of layer 6 connections have stabilized, the subplate is removed from the network as the newly developed layer 6 circuits become active. Simulations have shown that this new circuit is stable.

To demonstrate the importance of the subplate in the vertical development of interlaminar connections, a simulation was run without the influence of the subplate. In this simulation, layers 6 and 4 start off with random connection weights from the LGN. Maps of orientation and ocular dominance develop in both layers, but the maps are not coordinated. In addition, the layer 6-to-4 connections that develop are not vertical; see Figure 12B.

[Insert figure 12, about here]

Discussion

The cortical subplate is traditionally thought of as a transient cortical area underlying the cortical plate that is responsible for proper target recognition of developing thalamocortical connections. If the V1 subplate is ablated before the LGN growth cones contact cortex, the LGN efferents will grow past V1 and instead innervate other cortical areas (Ghosh and Shatz, 1993).

We predict that the subplate plays the equally important role of coordinating the development of cortical columns. This hypothesis is consistent with all the data known to us about early cortical development. For example, afferents from the LGN "wait" in the cortical subplate for a period of weeks before growing into the cortical plate (Ghosh and Shatz, 1992, 1994). If the subplate is ablated shortly after the LGN grows into layer 4, ocular dominance columns and orientation tuning (Ghosh and Shatz, 1992; Kanold et al., 2001) fail to develop. There exist reciprocal connections between the subplate and layer 4 (Ghosh, 1995). There also exist connections from the subplate to layer 1 (Allendoerfer and Shatz, 1994). Cells in layers 2/3 and 5 have apical dendrites in layer 1 (Callaway, 1998b). Connections also exist from most cortical layers to the subplate (Callaway, 1998b). Thus, circuits exist by which early activity in the cortical plate may be driven by the subplate.

The subplate contains sufficient circuitry to develop ocular dominance and orientation maps (Allendoerfer and Shatz, 1994); namely, lateral excitation and inhibition (see Figure 1), spontaneous inputs from the thalamus, and correlation learning (Grossberg and Olson, 1994). It is thus proposed that the subplate learns a map of orientation tuning and ocular dominance. When the LGN efferents grow into layer 4, the subplate also makes connections in layer 4 and correlations from the subplate guide the growth of the LGN-to-layer 4 connections and result in layer 4 developing the same map as found in the subplate. Likewise, the subplate is the main source of drive for layer 2/3, via the apical dendrites of the cells in layer 1, and the correlations from the subplate guide the clustering of horizontal connections in these layers. The fact that the subplate connects to all of the cortical layers results in vertical correlations that instruct the development of interlaminar connections. Once these interlaminar connections are in place, they are self-maintaining and when the subplate atrophies the developed cortical circuit remains stable.

Experiments are needed to verify these predictions. The model predicts that physiological recording of the subplate will reveal cells tuned for orientation. It also predicts that anatomical

staining will reveal ocular dominance columns in the subplate. Since the subplate atrophies shortly after eye opening, and is deep in cortex, there exists little physiological recording from this layer, but it is likely that cells are inadvertently recorded from the subplate and mistaken for layer 6 cells, which are orientationally tuned.

The model suggests how map loss after subplate ablation may be due to the resulting increase of BDNF in the cortical plate. It is possible that if the subplate is ablated, or inactivated, and the BDNF levels controlled, that maps of ocular dominance and orientation tuning might still form in cortex, since layers 4 and 6 have the same mechanisms supporting map formation as found in the subplate. We predict that, if this is verified, then vertical electrode penetrations would not initially find iso-oriented cells. Instead, while maps might still form in each cortical layer, they would be less coordinated across the layers.

We also predict that interlaminar connections that develop after the subplate is ablated would be less "vertical" than found in normal cortex. In the model, the vertical correlations provided by the subplate play an important role in the development of these interlaminar connections. In particular, the lateral correlations found in the horizontal layer 2/3 connections would drive the layer 4-to-2/3 connections in subplate-ablated cortex to be more scattered than in the normal animal.

Molecular and Activity-Based Mechanisms in Map Formation

It has been recently suggested that the initial specification of ocular dominance maps in the LGN and V1 is controlled by molecules expressed differently between the two eyes, or between the nasal and temporal regions of each eye. This hypothesis is supported by evidence that ocular dominance columns form in the cat at two weeks of age (Crowley and Katz, 1999, 2000), much earlier than first hypothesized and around the time that the LGN first innervates layer 4. Since Crowley and Katz did not eliminate the spontaneous activity between the LGN and subplate, they do not address the mechanisms used in our model. In fact, their data show eye-specific clusters of axons in the subplate before eye opening.

While some steps of visual map formation might be initially guided by activity-independent signals, such as ephrins (Cheng et al., 1995; Wilkinson, 2001), refined and complex patterning requires activity (Callaway and Katz, 1991; Cook et al., 1999; Dantzker and Callaway, 1998; Katz and Shatz, 1996; Penn et al., 1998; Weliky and Katz, 1997). Activity-based processing is needed if only to offset the lack of precision of the molecular map. On the scale of hundreds of microns, differences in the molecular gradients are too flat for exact target recognition. It may also be the case that maps related to visual features, such as orientation, are too specific for molecular patterning. Spontaneous activity may have evolved as the biological solution to efficient blueprinting. Later, patterned vision may refine these maps by optimizing them to fit environmental statistics, as well as individual differences in eye size and lateral separation. Binocular disparity tuning is a classical example of a process that depends on properties, like changing positions of the eyes in a growing head, that requires visual experience for final tuning (c.f., Grunewald and Grossberg, 1998).

Modeling Issues

Simulating development in the model requires running a large number of input iterations until the weights converge to a stable value. Each stage of the model required running 20,000-

100,000 iterations, and each iteration takes from 4 seconds to 1 minute to compute, depending on the number of layers and feedback connections. Each simulation thus takes from a day to a month to run on a 1.4 Ghz Athalon processor. Thus in order to carry out the full set of simulations, it was necessary to use a relatively small network of 26-by-26 cells for each layer.

While this model produces very good orientation tuning, the orientation map is not very smooth. The reason for this is the granularity of the network. Ocular dominance columns are only a few cells wide, which leaves no room for a full set of orientations. The granularity also introduces aliasing of isotropic filters, which has the result of producing an uneven distribution of orientations. A careful observer will note that there are a greater number of cells that prefer 45° and 135° than other angles. Since the model concerns how the orientation map is coordinated across layers, and not the fine-structure properties of such maps, and since fine resolution simulations of orientation maps that obey similar principles have been run elsewhere (e.g. Olson and Grossberg, 1998), our hypotheses are not compromised by these effects.

Conclusion

A model is proposed of how the cortical subplate learns a map of orientation and ocular dominance tuning and teaches this map to the other cortical layers via known anatomical connections. The model accounts for the coordination of orientation and ocular dominance maps, the coordination of ON and OFF subregions of simple cells receptive fields, the crude clustering of horizontal connections in layers 2/3, and the development of precise columns of coordinated receptive field properties across the multiple cortical layers. Related modeling work (Grossberg and Raizada, 2000; Grossberg and Williamson, 2001) supplements these results by showing how consistent laminar cortical mechanisms can account for the refinement of the horizontal connections in layer 2/3, develop a correct balance of excitation and inhibition within and between cortical layers, and explain neural recording during psychophysical experiments in adult animals.

References

Abbott LF, Varela JA, Sen K, Nelson SB (1997) Synaptic depression and cortical gain control. Science 275:220-224.

Albus K, Wolf W (1984) Early post-natal development of neuronal function in the kitten's visual cortex: a laminar analysis. J Physiol 348:153-185.

Allendoerfer KL, Shatz CJ (1994) The subplate, a transient neocortical structure: its role in the development of connections between thalamus and cortex. Annu Rev Neurosci 17:185-218.

Alonso JM, Usrey WM, Reid RC (2001) Rules of connectivity between geniculate cells and simple cells in cat primary visual cortex. J Neurosci 21:4002-4015.

Anderson JS, Lampl I, Gillespie DC, Ferster D (2000) The contribution of noise to contrast invariance of orientation tuning in cat visual cortex [In Process Citation]. Science 290:1968-1972.

Berardi N, Maffei L (1999) From visual experience to visual function: roles of neurotrophins. J Neurobiol 41:119-126.

Blasdel GG (1992a) Orientation selectivity, preference, and continuity in monkey striate cortex. J Neurosci 12:3139-3161.

Blasdel GG (1992b) Differential imaging of ocular dominance and orientation selectivity in monkey striate cortex. J Neurosci 12:3115-3138.

Bosking WH, Zhang Y, Schofield B, Fitzpatrick D (1997) Orientation selectivity and the arrangement of horizontal connections in tree shrew striate cortex. J Neurosci 17:2112-2127.

Brodmann K (1909) Vergleichende Lokalisationslehre der Grosshirnrinde in ihren Prinzipien dargestellt auf Grund des Zellenbaues. Leipzig,.

Cabelli RJ, Hohn A, Shatz CJ (1995) Inhibition of ocular dominance column formation by infusion of NT-4/5 or BDNF. Science 267:1662-1666.

Cabelli RJ, Shelton DL, Segal RA, Shatz CJ (1997) Blockade of endogenous ligands of trkB inhibits formation of ocular dominance columns. Neuron 19:63-76.

Callaway EM (1998a) Local circuits in primary visual cortex of the macaque monkey. Annu Rev Neurosci 21:47-74.

Callaway EM (1998b) Prenatal development of layer-specific local circuits in primary visual cortex of the macaque monkey. J Neurosci 18:1505-1527.

Callaway EM, Katz LC (1990) Emergence and refinement of clustered horizontal connections in cat striate cortex. J Neurosci 10:1134-1153.

Callaway EM, Katz LC (1991) Effects of binocular deprivation on the development of clustered horizontal connections in cat striate cortex. Proc Natl Acad Sci U S A 88:745-749.

Callaway EM, Katz LC (1992) Development of axonal arbors of layer 4 spiny neurons in cat striate cortex. J Neurosci 12:570-582.

Carandini M, Ringach DL (1997) Predictions of a recurrent model of orientation selectivity. Vision Res 37:3061-3071.

Carpenter GA, Grossberg S (1987) ART 2: Self-organization of stable category recognition codes for analog input patterns. In: Proceedings of the IEEE international conference on neural networks (Butler MCaC, ed), pp 727-736.

Chakrabarty S, Martin JH (2000) Postnatal development of the motor representation in primary motor cortex. J Neurophysiol 84:2582-2594.

Chapman B, Zahs KR, Stryker MP (1991) Relation of cortical cell orientation selectivity to alignment of receptive fields of the geniculocortical afferents that arborize within a single orientation column in ferret visual cortex. J Neurosci 11:1347-1358.

Cheng HJ, Nakamoto M, Bergemann AD, Flanagan JG (1995) Complementary gradients in expression and binding of ELF-1 and Mek4 in development of the topographic retinotectal projection map. Cell 82:371-381.

Cook PM, Prusky G, Ramoa AS (1999) The role of spontaneous retinal activity before eye opening in the maturation of form and function in the retinogeniculate pathway of the ferret. Vis Neurosci 16:491-501.

Crair MC, Gillespie DC, Stryker MP (1998) The role of visual experience in the development of columns in cat visual cortex. Science 279:566-570.

Crair MC, Horton JC, Antonini A, Stryker MP (2001) Emergence of ocular dominance columns in cat visual cortex by 2 weeks of age. J Comp Neurol 430:235-249.

Crair MC, Ruthazer ES, Gillespie DC, Stryker MP (1997a) Ocular dominance peaks at pinwheel center singularities of the orientation map in cat visual cortex. J Neurophysiol 77:3381-3385.

Crair MC, Ruthazer ES, Gillespie DC, Stryker MP (1997b) Relationship between the ocular dominance and orientation maps in visual cortex of monocularly deprived cats. Neuron 19:307-318.

Crowley JC, Katz LC (1999) Development of ocular dominance columns in the absence of retinal input. Nat Neurosci 2:1125-1130.

Crowley JC, Katz LC (2000) Early development of ocular dominance columns. Science 290:1321-1324.

Dantzker JL, Callaway EM (1998) The development of local, layer-specific visual cortical axons in the absence of extrinsic influences and intrinsic activity. J Neurosci 18:4145-4154.

Donoghue MJ, Rakic P (1999) Molecular gradients and compartments in the embryonic primate cerebral cortex. Cereb Cortex 9:586-600.

Duffy KR, Murphy KM, Jones DG (1998) Analysis of the postnatal growth of visual cortex. Vis Neurosci 15:831-839.

Durbin R, Mitchison G (1990) A dimension reduction framework for understanding cortical maps. Nature 343:644-647.

Dykes RW, Rasmusson DD, Hoeltzell PB (1980) Organization of primary somatosensory cortex in the cat. J Neurophysiol 43:1527-1546.

Elliott T, Shadbolt NR (1999) A neurotrophic model of the development of the retinogeniculocortical pathway induced by spontaneous retinal waves. J Neurosci 19:7951-7970.

Ferster D, Miller KD (2000) Neural mechanisms of orientation selectivity in the visual cortex. Annu Rev Neurosci 23:441-471.

Fitzpatrick D, Lund JS, Blasdel GG (1985) Intrinsic connections of macaque striate cortex: afferent and efferent connections of lamina 4C. J Neurosci 5:3329-3349.

Galuske RA, Singer W (1996) The origin and topography of long-range intrinsic projections in cat visual cortex: a developmental study. Cereb Cortex 6:417-430.

Gaudiano P, Grossberg S (1991) Vector Associative Maps: Unsupervised real-time error-based learning and control of movement trajectories. Neural Networks 4:147-183.

Ghosh A (1995) Subplate Neurons And The Patterning Of Thalamocortical Connections. In: Ciba Foundation symposium ; 193, 193 Edition (Bock G, Cardew G, eds), pp 150-165. Chichester ; New York: J. Wiley.

Ghosh A, Shatz CJ (1992) Involvement of subplate neurons in the formation of ocular dominance columns. Science 255:1441-1443.

Ghosh A, Shatz CJ (1993) A role for subplate neurons in the patterning of connections from thalamus to neocortex. Development 117:1031-1047.

Ghosh A, Shatz CJ (1994) Segregation of geniculocortical afferents during the critical period: a role for subplate neurons. J Neurosci 14:3862-3880.

Gilbert CD, Wiesel TN (1983) Clustered intrinsic connections in cat visual cortex. J Neurosci 3:1116-1133.

Gilbert CD, Wiesel TN (1985) Intrinsic connectivity and receptive field properties in visual cortex. Vision Res 25:365-374.

Gilbert CD, Wiesel TN (1989) Columnar specificity of intrinsic horizontal and corticocortical connections in cat visual cortex. J Neurosci 9:2432-2442.

Grinvald A, Lieke E, Frostig RD, Gilbert CD, Wiesel TN (1986) Functional architecture of cortex revealed by optical imaging of intrinsic signals. Nature 324:361-364.

Grossberg S (1968) Some physiological and biochemical consequences of psychological postulates. Proc Natl Acad Sci U S A:758-765.

Grossberg S (1973) Contour enhancement, short term memory, and constancies in reverberating neural networks. Studies in Applied Mathematics 52: 217-257.

Grossberg S (1976) Adaptive pattern classification and universal recoding. I. Parallel development and coding of neural feature detectors. Biological Cybernetics 23:121–134.

Grossberg S (1980) How does a brain build a cognitive code? Psychol Rev 87:1-51.

Grossberg S (1994) 3-D vision and figure-ground separation by visual cortex. Percept Psychophys 55:48-121.

Grossberg S (1997) Cortical dynamics of three-dimensional figure-ground perception of two-dimensional pictures. Psychol Rev 104:618-658.

Grossberg S, Hwang S, Mingolla E (2002) Thalamocortical dynamics of the McCollough effect: Boundary-surface alignment through perceptual learning. Vision Res in press.

Grossberg S, Mcloughlin NP (1997) Cortical dynamics of three-dimensional surface perception - binocular and half-occluded scenic images. Neural Networks 10:1583-1605.

Grossberg S, Mingolla E (1985) Neural dynamics of perceptual grouping: textures, boundaries, and emergent segmentations. Percept Psychophys 38:141-171.

Grossberg S, Olson S (1994) Rules for the Cortical Map of Ocular Dominance and Orientation Columns. Neural Networks 7:883-984.

Grossberg S, Raizada RD (2000) Contrast-sensitive perceptual grouping and object-based attention in the laminar circuits of primary visual cortex. Vision Res 40:1413-1432.

Grossberg S, Williamson JR (2001) A neural model of how horizontal and interlaminar connections of visual cortex develop into adult circuits that carry out perceptual grouping and learning. Cereb Cortex 11:37-58.

Grunewald A, Grossberg S (1998) Self-organization of binocular disparity tuning by reciprocal corticogeniculate interactions. J Cogn Neurosci 10:199-215.

Hodgkin AL, Huxley AF (1952) A quantitative description of membrane current and its application to conduction and excitation in nerve. Journal of Physiology London 117:500-544.

Hubel DH, Wiesel TN (1959) Receptive fields of single neurones in the cat's striate cortex. J

Physiol 148:574-591.

Hubel DH, Wiesel TN (1962) Receptive fields, binocular interaction and functional architecture in the cat's visual cortex. Journal of Physiology London 160.

Hubener M, Shoham D, Grinvald A, Bonhoeffer T (1997) Spatial relationships among three columnar systems in cat area 17. J Neurosci 17:9270-9284.

Kanold PO, Kara P, Reid RC, Shatz CJ (2001) Requirement for subplate neurons in functional maturation of visual cortex. Soc Neurosci Abstr 31:27.16.

Kaplan E, Purpura K, Shapley RM (1987) Contrast affects the transmission of visual information through the mammalian lateral geniculate nucleus. J Physiol 391:267-288.

Katz LC, Gilbert CD, Wiesel TN (1989) Local circuits and ocular dominance columns in monkey striate cortex. J Neurosci 9:1389-1399.

Katz LC, Shatz CJ (1996) Synaptic activity and the construction of cortical circuits. Science 274:1133-1138.

Kohonen T (1982) Self-organized formation of topologically correct feature maps. Biological Cybernetics 43:59–69.

Komiya H, Eggermont JJ (2000) Spontaneous firing activity of cortical neurons in adult cats with reorganized tonotopic map following pure-tone trauma. Acta Otolaryngol 120:750-756.

Linsker R (1986a) From basic network principles to neural architecture: emergence of orientation columns. Proc Natl Acad Sci U S A 83:8779-8783.

Linsker R (1986b) From basic network principles to neural architecture: emergence of orientation-selective cells. Proc Natl Acad Sci U S A 83:8390-8394.

Linsker R (1986c) From basic network principles to neural architecture: emergence of spatial-opponent cells. Proc Natl Acad Sci U S A 83:7508-7512.

Lowel S, Singer W (1992) Selection of intrinsic horizontal connections in the visual cortex by correlated neuronal activity. Science 255:209-212.

Lund JS, Wu Q, Hadingham PT, Levitt JB (1995) Cells and circuits contributing to functional properties in area V1 of macaque monkey cerebral cortex: bases for neuroanatomically realistic models. J Anat 187 (Pt 3):563-581.

Luskin MB, Shatz CJ (1985) Studies of the earliest generated cells of the cat's visual cortex: cogeneration of subplate and marginal zones. J Neurosci 5:1062-1075.

Markram H, Tsodyks M (1996) Redistribution of synaptic efficacy between neocortical pyramidal neurons. Nature 382:807-810.

Maunsell JH, Ghose GM, Assad JA, McAdams CJ, Boudreau CE, Noerager BD (1999) Visual response latencies of magnocellular and parvocellular LGN neurons in macaque monkeys. Vis Neurosci 16:1-14.

McAllister AK (1999) Subplate neurons: a missing link among neurotrophins, activity, and ocular dominance plasticity? Proc Natl Acad Sci U S A 96:13600-13602.

McAllister AK, Katz LC, Lo DC (1997) Opposing roles for endogenous BDNF and NT-3 in regulating cortical dendritic growth. Neuron 18:767-778.

McConnell SK, Ghosh A, Shatz CJ (1994) Subplate pioneers and the formation of descending connections from cerebral cortex. J Neurosci 14:1892-1907.

McConnell SK, Kaznowski CE (1991) Cell cycle dependence of laminar determination in developing neocortex. Science 254:282-285.

McGuire BA, Gilbert CD, Rivlin PK, Wiesel TN (1991) Targets of horizontal connections in macaque primary visual cortex. J Comp Neurol 305:370-392.

Miller KD (1992) Development of orientation columns via competition between ON- and OFF-center inputs. Neuroreport 3:73-76.

Miller KD, Keller JB, Stryker MP (1989) Ocular dominance column development: analysis and simulation. Science 245:605-615.

Munoz DP, Pelisson D, Guitton D (1991) Movement of neural activity on the superior colliculus motor map during gaze shifts. Science 251:1358-1360.

Murphy PC, Duckett SG, Sillito AM (1999) Feedback connections to the lateral geniculate nucleus and cortical response properties. Science 286:1552-1554.

Nieoullon A, Rispal-Padel L (1976) Somatotopic localization in cat motor cortex. Brain Res 105:405-422.

Obermayer K, Blasdel GG (1993) Geometry of orientation and ocular dominance columns in monkey striate cortex. J Neurosci 13:4114-4129.

Obermayer K, Blasdel GG, Schulten K (1992) Statistical-mechanical analysis of self-organization and pattern formation during the development of visual maps. Physical Review A 45:7568-7589.

Olson S, Grossberg S (1998) A neural network model for the development of simple and complex cell receptive fields within cortical maps of orientation and ocular dominance. Neural Networks 11:189–208.

Papaioannou J, White A (1972) Maintained activity of lateral geniculate nucleus neurons as a function of background luminance. Exp Neurol 34:558-566.

Penn AA, Riquelme PA, Feller MB, Shatz CJ (1998) Competition in retinogeniculate patterning driven by spontaneous activity. Science 279:2108-2112.

Purves D (1988) Body and brain : a trophic theory of neural connections. Cambridge, Mass.: Harvard University Press.

Reid RC, Alonso JM (1995) Specificity of monosynaptic connections from thalamus to visual cortex. Nature 378:281-284.

Rojer AS, Schwartz EL (1990) Cat and monkey cortical columnar patterns modeled by bandpass-filtered 2D white noise. Biol Cybern 62:381-391.

Ruthazer ES, Stryker MP (1996) The role of activity in the development of long-range horizontal connections in area 17 of the ferret. J Neurosci 16:7253-7269.

Schmidt KE, Galuske RA, Singer W (1999) Matching the modules: cortical maps and long-range intrinsic connections in visual cortex during development. J Neurobiol 41:10-17.

Schmidt KE, Goebel R, Lowel S, Singer W (1997a) The perceptual grouping criterion of colinearity

is reflected by anisotropies of connections in the primary visual cortex. Eur J Neurosci 9:1083-1089.

Schmidt KE, Kim DS, Singer W, Bonhoeffer T, Lowel S (1997b) Functional specificity of long-range intrinsic and interhemispheric connections in the visual cortex of strabismic cats. J Neurosci 17:5480-5492.

Sclar G, Ohzawa I, Freeman RD (1985) Contrast gain control in the kitten's visual system. J Neurophysiol 54:668-675.

Seitz A, Grossberg S (2001) Coordination of Laminar Development in V1 by the Cortical Subplate. Soc Neurosci Abstr 31:619.

Seitz A, Grossberg S (2002) How Do Laminar Circuits Develop? The Role of the Cortical Subplate in the Development and Laminar Coordination of Orientation and Ocular Dominance Maps in V1. Vis Sci Soc Abstr 2:40.

Shatz CJ, Lindstrom S, Wiesel TN (1977) The distribution of afferents representing the right and left eyes in the cat's visual cortex. Brain Res 131:103-116.

Sincich LC, Blasdel GG (2001) Oriented axon projections in primary visual cortex of the monkey. J Neurosci 21:4416-4426.

Sirosh J, Miikkulainen R (1997) Topographic receptive fields and patterned lateral interaction in a self-organizing model of the primary visual cortex. Neural Comput 9:577-594.

Skottun BC, Bradley A, Sclar G, Ohzawa I, Freeman RD (1987) The effects of contrast on visual orientation and spatial frequency discrimination: a comparison of single cells and behavior. J Neurophysiol 57:773-786.

Stanton SG, Harrison RV (2000) Projections from the medial geniculate body to primary auditory cortex in neonatally deafened cats. J Comp Neurol 426:117-129.

Swindale NV (1980) A model for the formation of ocular dominance stripes. Proc R Soc Lond B Biol Sci 208:243-264.

Swindale NV (1992) A model for the coordinated development of columnar systems in primate striate cortex. Biol Cybern 66:217-230.

Tootell RB, Hadjikhani NK, Vanduffel W, Liu AK, Mendola JD, Sereno MI, Dale AM (1998) Functional analysis of primary visual cortex (V1) in humans. Proc Natl Acad Sci U S A 95:811-817.

Tootell RB, Silverman MS, Switkes E, De Valois RL (1982) Deoxyglucose analysis of retinotopic organization in primate striate cortex. Science 218:902-904.

Ts'o DY, Gilbert CD, Wiesel TN (1986) Relationships between horizontal interactions and functional architecture in cat striate cortex as revealed by cross-correlation analysis. J Neurosci 6:1160-1170.

von der Malsburg C (1973) Self-organization of orientation sensitive cells in the striate cortex. Kybernetik 14:85-100.

Wallace MT, Stein BE (1996) Sensory organization of the superior colliculus in cat and monkey. Prog Brain Res 112:301-311.

Weliky M, Katz LC (1997) Disruption of orientation tuning in visual cortex by artificially

correlated neuronal activity. Nature 386:680-685.

Weliky M, Katz LC (1999) Correlational structure of spontaneous neuronal activity in the developing lateral geniculate nucleus in vivo. Science 285:599-604.

Wilkinson DG (2001) Multiple roles of EPH receptors and ephrins in neural development. Nat Rev Neurosci 2:155-164.

Willshaw DJ, von der Malsburg C (1976) How patterned neural connections can be set up by self-organization. Proc R Soc Lond B Biol Sci 194:431-445.

Wong RO, Oakley DM (1996) Changing patterns of spontaneous bursting activity of on and off retinal ganglion cells during development. Neuron 16:1087-1095.

Yoshioka T, Blasdel GG, Levitt JB, Lund JS (1996) Relation between patterns of intrinsic lateral connectivity, ocular dominance, and cytochrome oxidase-reactive regions in macaque monkey striate cortex. Cereb Cortex 6:297-310.

Figures

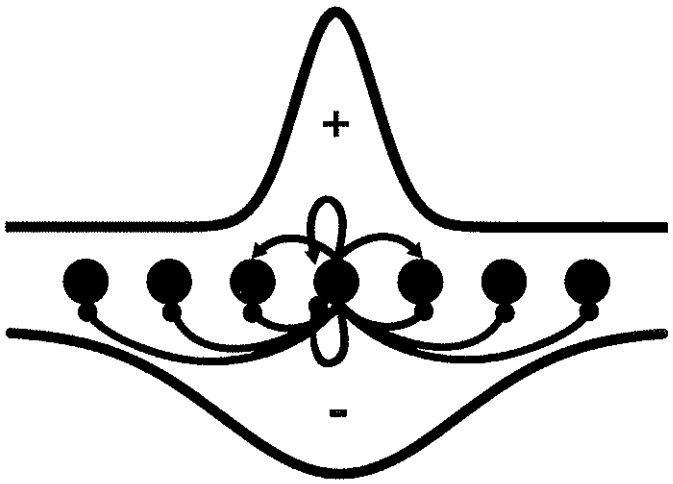

Figure 1 – Circuit for local excitatory and inhibitory connections. A normalized Difference-of-Gaussian, or bandpass, filter is realized through local short-range excitatory connections, arrows on top, and longer-range inhibitory connections, circles on bottom, in a network whose cells obey membrane equations. This basic circuit exists in each of the model layers that are depicted in Figure 2.

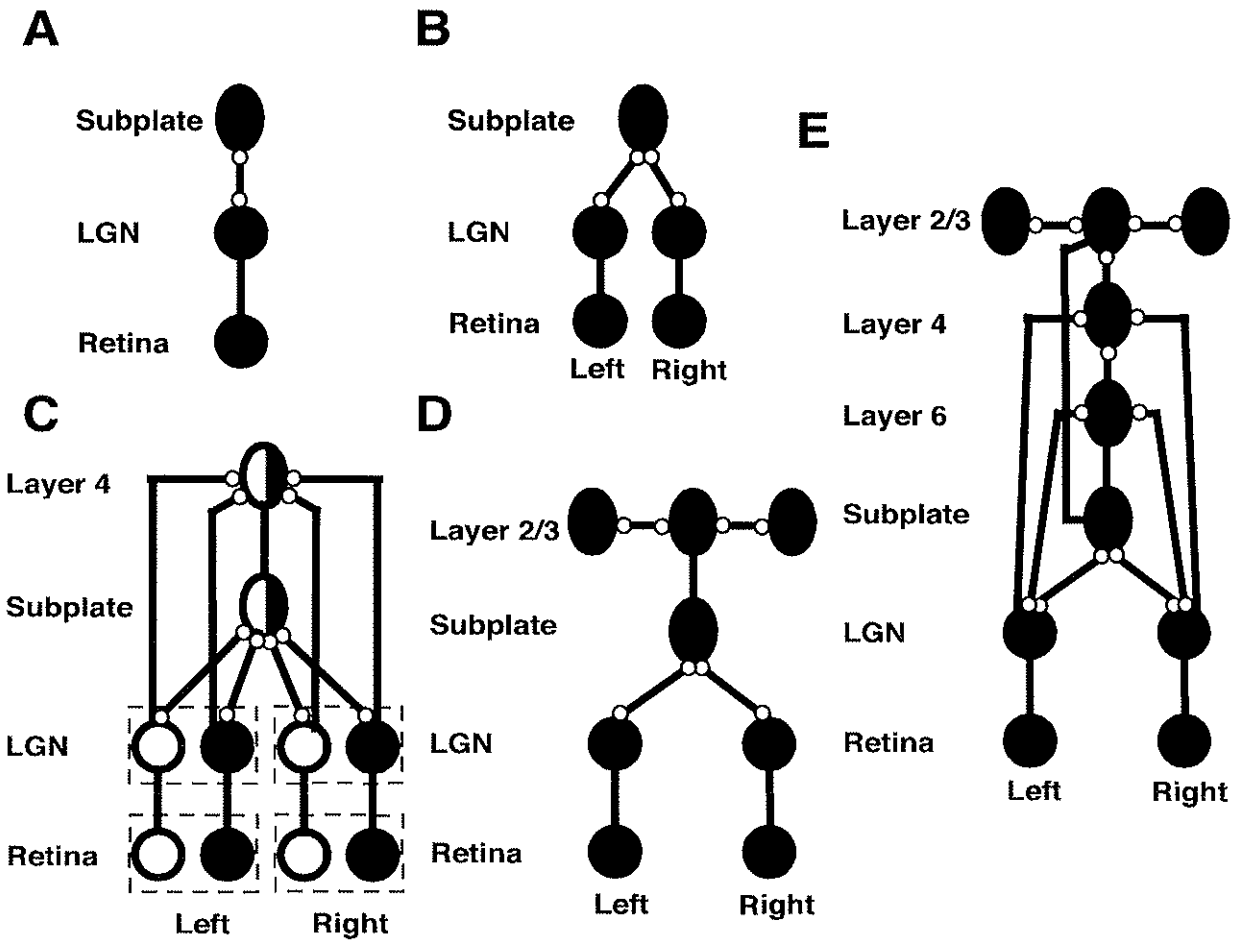

Figure 2 – Diagram of different model stages. A: Monocular subplate circuit. Spontaneous activity in retinal OFF cells drives the LGN, which inputs to the subplate. Feedforward weights from the subplate and feedback weights to the LGN develop into a map of oriented receptive fields. B: Binocular subplate circuit. Here input from a second eye is introduced and a map of ocular dominance develops in the subplate, superimposed on the existing orientation map. C: Binocular layer 4 circuit. Here the orientation and ocular dominance maps that exist in the subplate are taught to layer 4. In a subsequent simulation, ON retinal ganglion cells are introduced and patterned retinal inputs provide correlations that help to segregate ON and OFF subfields in layer 4. D: Layer 2/3 circuit. Here clusters of horizontal connections develop in layer 2/3 guided by the correlations provided by the subplate. E: Circuit of the fully developed model. Here layer 6 is introduced, which develops connections to and from the LGN. Then interlaminar connections are developed from layer 6 to layer 4 and from layer 4 to layer 2/3. Finally the inputs to and from the subplate are removed and the model is shown to be stable. In all figures, black circles denote OFF receptive fields, white circles denote ON receptive fields, ovals denote orientationally tuned cells, lines ending in open circles denote plastic connections. Lines without circles denote feedforward non-additive connections.

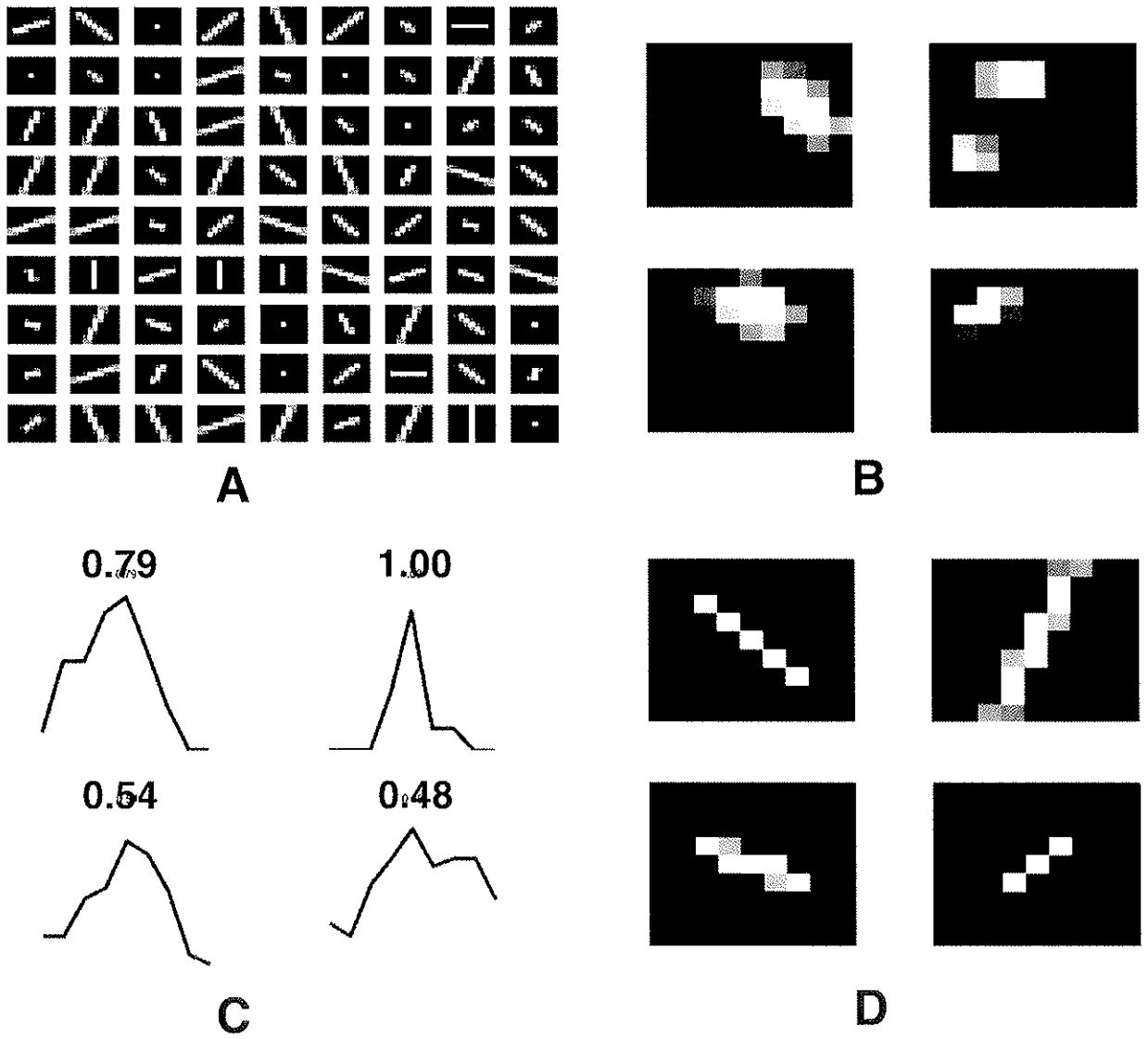

Figure 3 – Development of orientation tuning in the monocular subplate circuit; see Figure 2A. A: Summary of orientation tuning for a 9-by-9 grid of cells in the center of the subplate layer. Each block represents a single cell and portrays that cell's preferred orientation and degree of tuning, as detailed in B-D. B: Raw receptive fields for 4 typical cells. C: Orientation tuning curves, for cells in B, produced by probing the network, at each spatial location, with bars of 8 different orientations and plotting the peak response to each orientation. The number above each curve is the orientation index (difference between peak and null orientations divided by sum) for each cell. D: For each cell, the line corresponding to the peak orientation, from C, is drawn with length proportional to the orientation index.

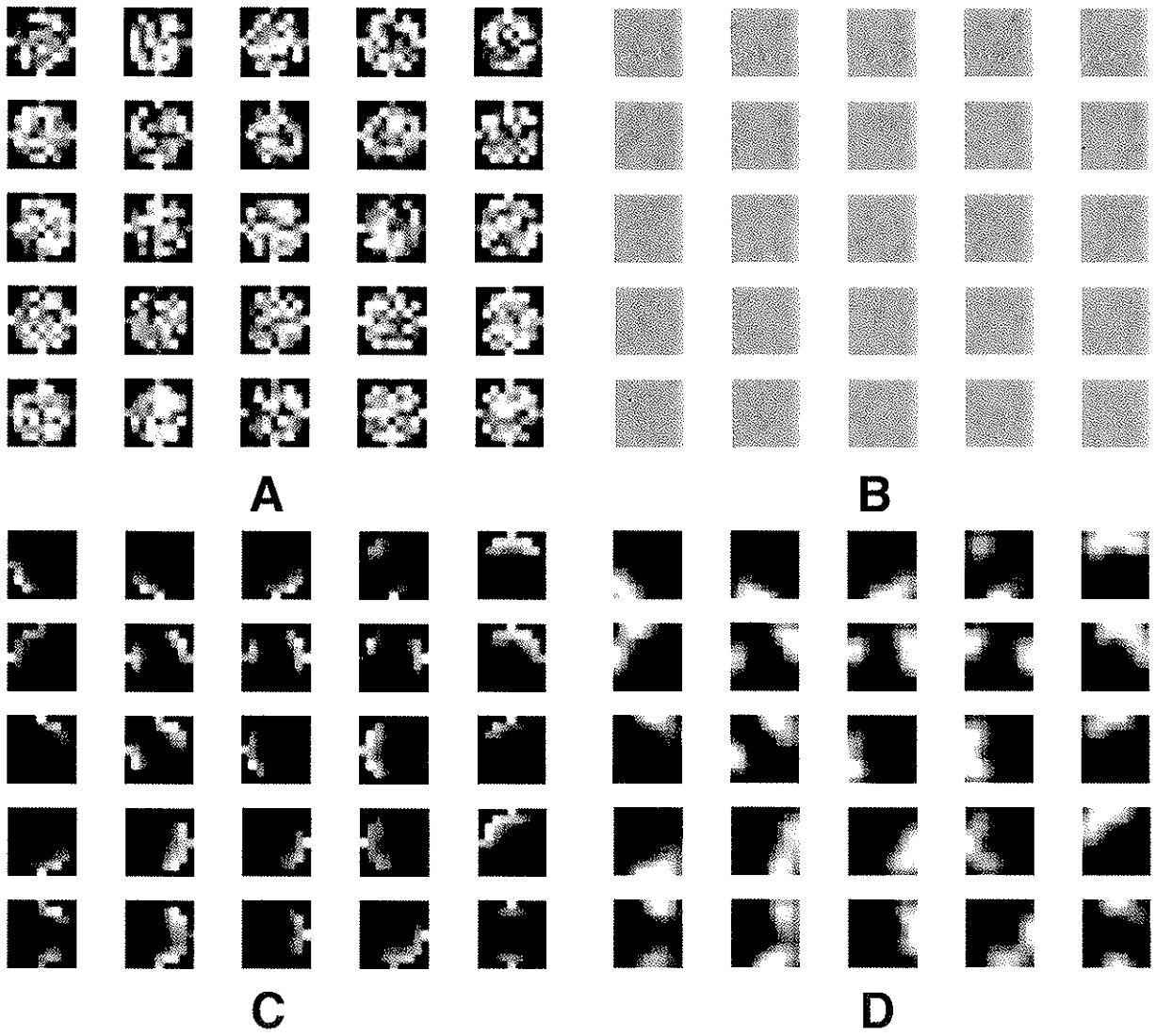

Figure 4 – Pattern of feedforward and feedback connections between the LGN and subplate before and after learning. A: Initial weight profiles from the LGN to subplate are generated as white spatial noise with limited spatial extent. B: Initial weight profiles from the subplate to LGN are initially uniform and equal to 1. C: After learning, weights from the LGN to subplate are refined and oriented. D: After learning, weights from subplate to LGN are patterned and are oriented in the same manner as the equivalent LGN-to-subplate weights.

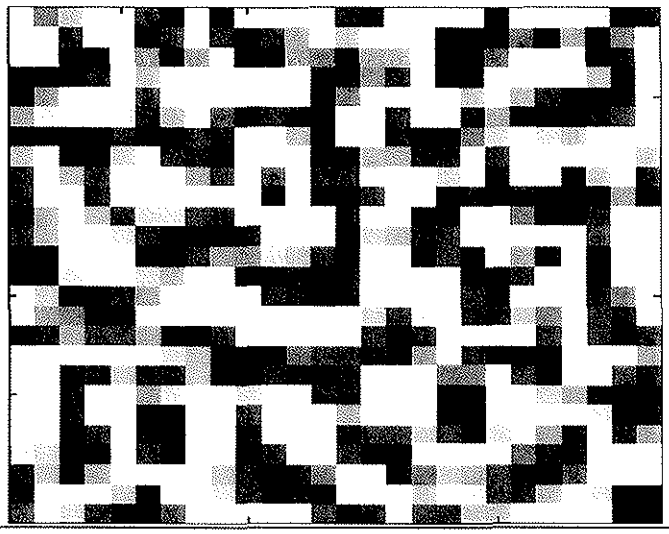

Figure 5 – Ocular dominance columns in the subplate; see figure 2B. Plotted is the ocularity index (the difference between the ipsilateral and contralateral weights divided by the sum). This plot shows the ocular dominance across the entire subplate layer. Each pixel represents the ocular dominance of an individual subplate cell.

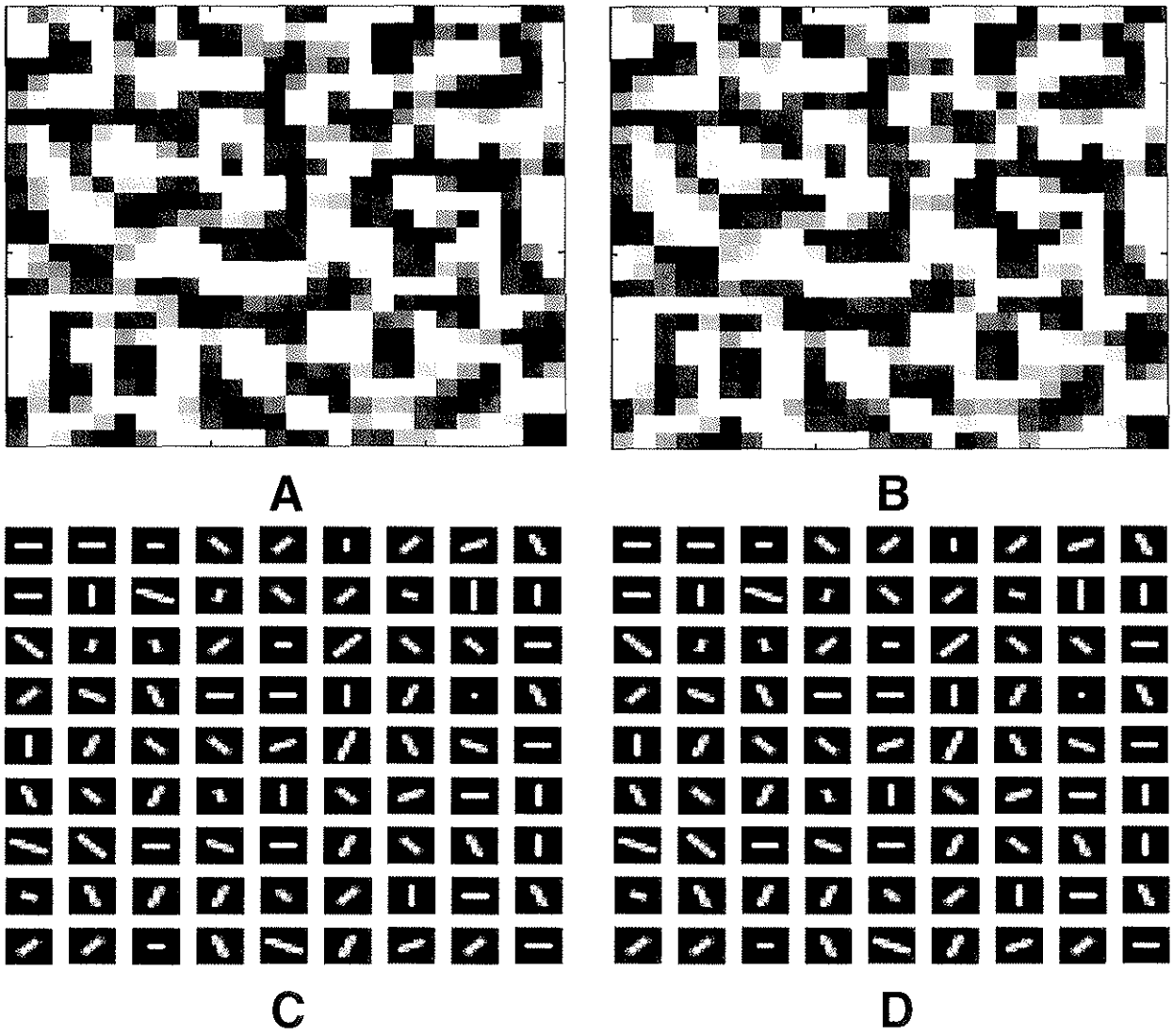

Figure 6 – Ocular dominance columns and orientation preferences in the subplate and layer 4; see Figure 2C. A: Ocular dominance columns in the subplate. B: Nearly identical ocular dominance columns in layer 4. C: Orientation preferences in the subplate. D: Nearly identical orientation preferences in layer 4. Ocular dominance is shown for the entire 26-by-26 network, orientation for a 9-by-9 subset.

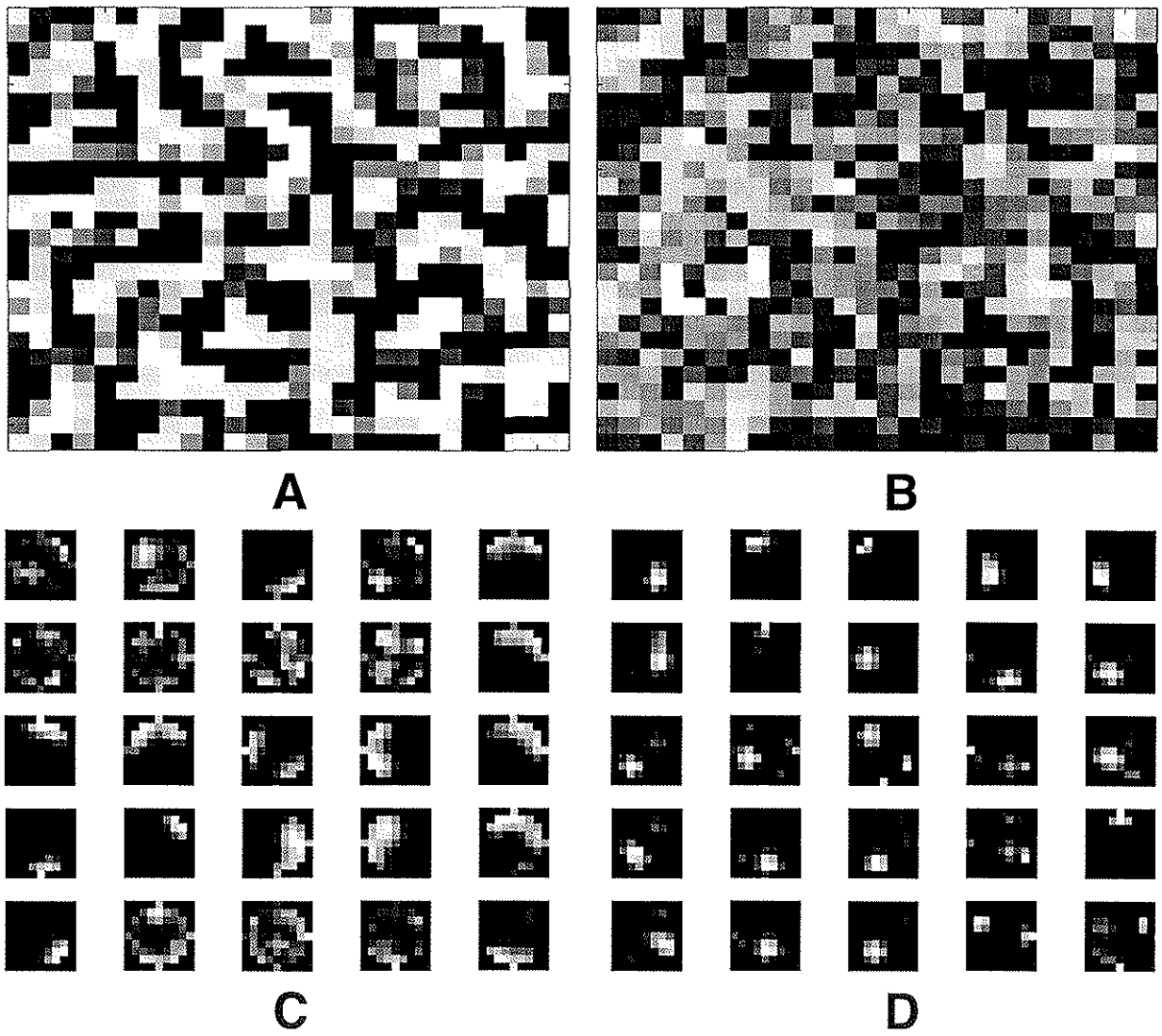

Figure 7 – Connection weights and ocular dominance columns when $J^{(4)}$ is decreased. A and C: Ocular dominance columns and contralateral eye receptive field profiles for $J^{(4)} = 1$. In C, the receptive fields profiles that are unpatterned correspond to cells dominated by the ipsilateral eye. B and D: No ocular dominance columns and less oriented receptive field profiles when $J^{(4)} = 0.1$.

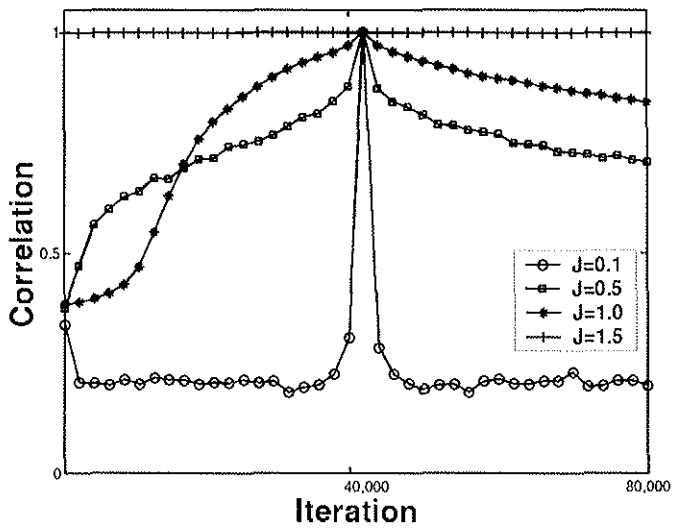

Figure 8 – Stability of weights when $J^{(4)}$ is varied. Plotted is the pixel-by-pixel correlation between the weights at each time point and those of iteration 40,000, for different values of $J^{(4)}$. $J^{(4)} = 1$: These weights are the most stable and, once the weights converge, there is only a slow variation of the weights. $J^{(4)} = 0.5$: Weights develop more rapidly, but also are less stable. $J^{(4)} = 0.1$: Weights are extremely unstable. $J^{(4)} = 1.5$: Weights do not develop significantly from initial values. This last case is consistent with experiments about subplate ablation.

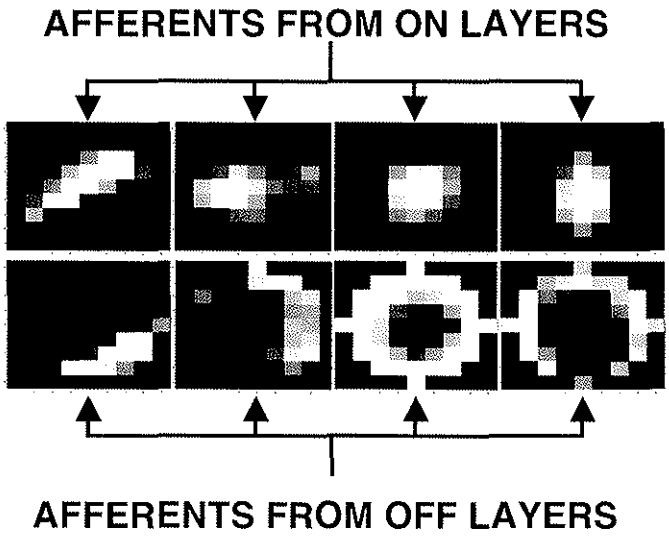

Figure 9 – Patterned vision segregates ON and OFF subfields in layer 4; see Figure 2C. Top row shows the patterns of connection strength from the ON LGN layer to four representative layer 4 cells. Bottom row shows the patterns of connection strength from the OFF LGN layer to the same cells. Note that the ON and OFF layers are segregated. As is found in vivo, both even and odd symmetric cell types develop.

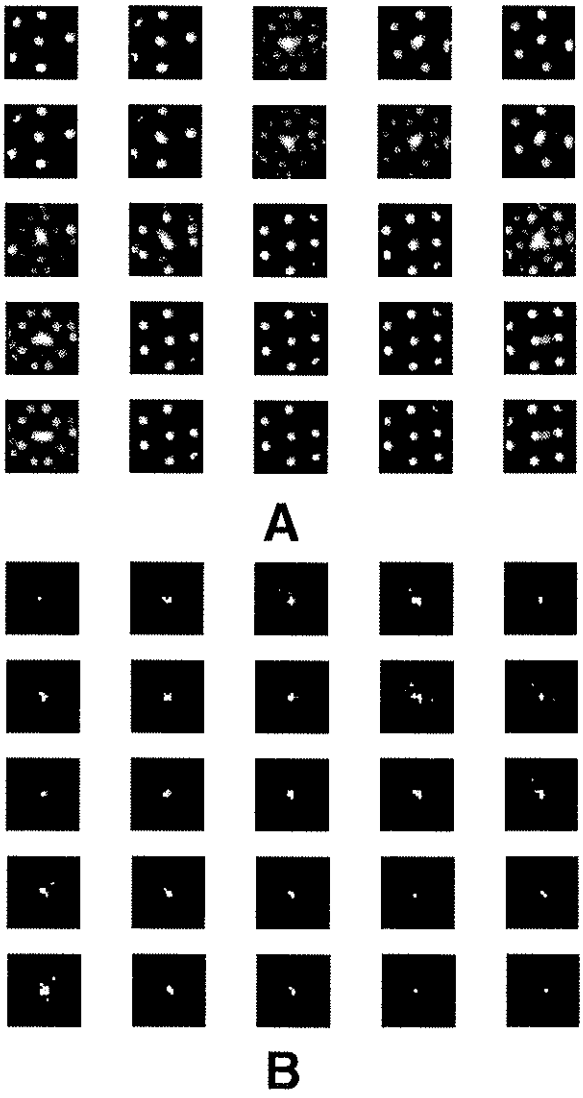

Figure 10 – Pattern of connections for layer 2/3 simulation; see Figure 2D. Each block shows the pattern of connections to a different layer 2/3 cell. The patterns of connections are centered on the location of each cell. A: Clustered horizontal connections between layer 2/3 cells. B: Learned interlaminar connections from layer 4 to layer 2/3.

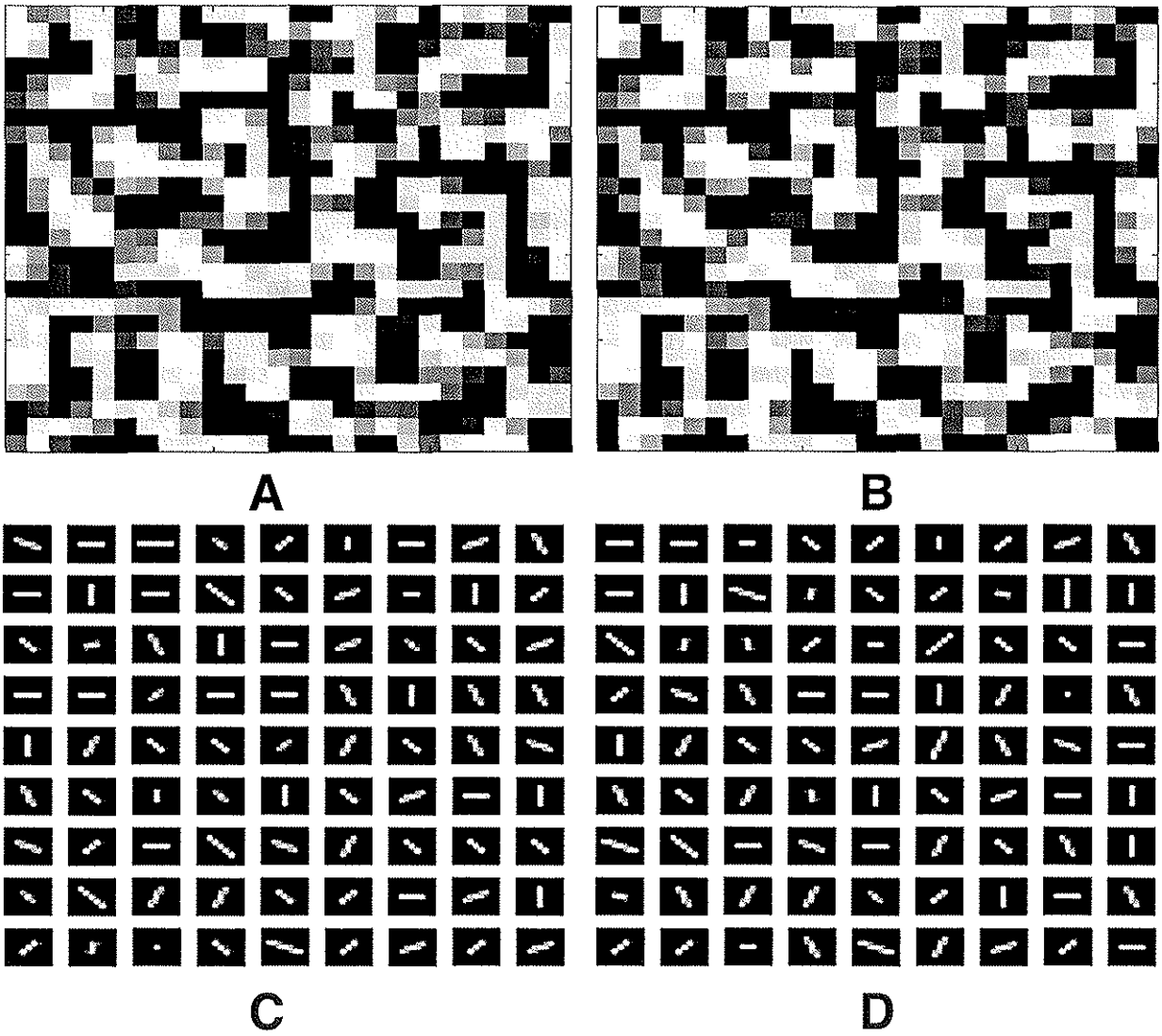

Figure 11 – Ocular dominance columns and orientation preferences in layer 6 and layer 4; see Figure 2E. A: Ocular dominance columns in layer 4. B: Nearly identical columns in layer 6. C: Orientation preferences in layer 4. D: Nearly identical preferences in layer 6.

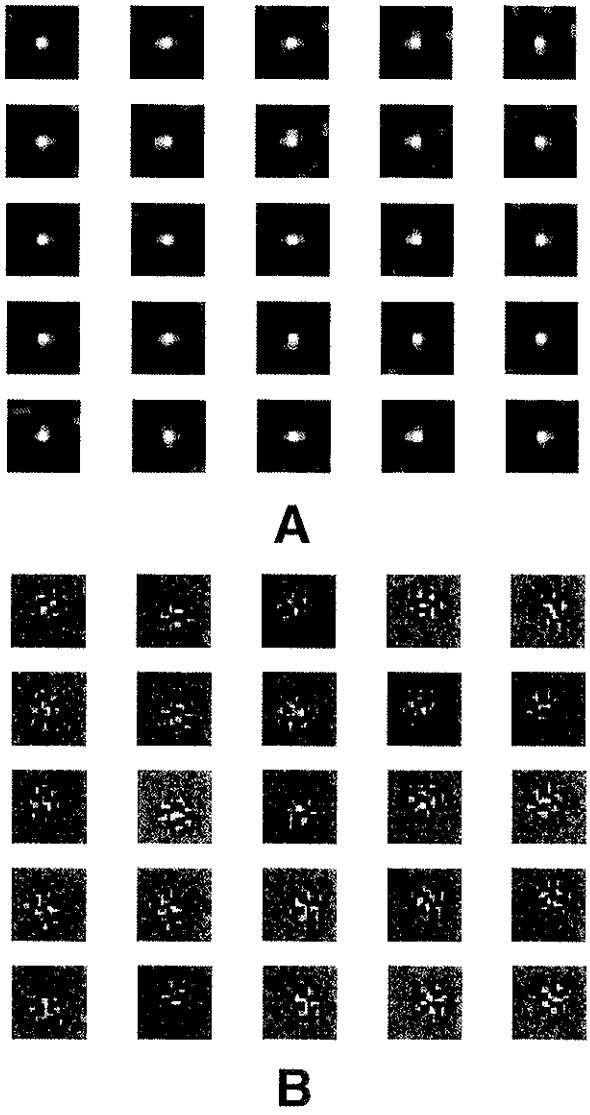

Figure 12 - Learned connections from layer 6 to layer 4. A: Normally forming interlaminar connections are vertical. B: Subplate is ablated before interlaminar connections develop. As a result layer 6-to-4 connections do not develop vertically.